processes

MDPI

Article

Advancing Towards Zero Liquid Discharge: Hybrid Membrane and Electro-Oxidation Processes for Petrochemical Wastewater Reuse

Éverton Hansen [1,2], Marcos Vinícius Tenedini [1], Andréia Barros dos Santos [3], Patrice Monteiro De Aquim [3], Salatiel Wohlmuth da Silva [4], Alexey Volkov [5], Andréa Moura Bernardes [6,*,†] and Marco Antônio Siqueira Rodrigues [1,3]

1 Post-Graduation Program in Environmental Quality, Feevale University, Novo Hamburgo 93525-075, RS, Brazil; evertonhansen@gmail.com (É.H.); marcos.tenedini@yahoo.com (M.V.T.); marcor@feevale.br (M.A.S.R.)
2 State Foundation for Environmental Protection—FEPAM, Porto Alegre 90020-021, RS, Brazil
3 Post-Graduation Program in Materials Technology and Industrial Processes, Feevale University, Novo Hamburgo 93525-075, RS, Brazil; andreia.cetel@gmail.com (A.B.d.S.); patrice@feevale.br (P.M.D.A.)
4 Post-Graduation Program in Water Resources and Environmental Sanitation, Federal University of Rio Grande do Sul UFRGS, Porto Alegre 91509-900, RS, Brazil; salatiel.silva@ufrgs.br
5 A.V. Topchiev Institute of Petrochemical Synthesis (TIPS RAS), Russian Academy of Sciences, Moscow 119991, Russia; avolkov@ips.ac.ru
6 Post-Graduation Program in Mining, Metallurgical and Materials Engineering (PPGE3M), Federal University of Rio Grande do Sul (UFRGS), Porto Alegre 91509-900, RS, Brazil
* Correspondence: amb@ufrgs.br
† Permanent address: Departamento de Materiais, Escola de Engenharia, Campus do Vale Setor IV—Prédio 74, Universidade Federal do Rio Grande do Sul, Av. Bento Gonçalves, 9500, Bairro Agronomia, Porto Alegre 91501-970, RS, Brazil.

Abstract

Petrochemical industries consume substantial volumes of water and generate complex wastewaters that require advanced treatment to enable sustainable reuse. This study developed and evaluated a hybrid treatment system integrating ultrafiltration (UF), reverse osmosis (RO), electrodeionization (EDI), membrane distillation (MD), and electro-oxidation (EO) for tertiary petrochemical wastewater recovery and reuse. Pilot-scale UF achieved 91.5% water recovery, effectively removing suspended solids, turbidity, and iron, thereby producing suitable feedwater for downstream RO treatment. The RO system operated at 50.5% water recovery, generating permeate, with conductivity below 40 µS/cm for EDI polishing, and concentrate streams for MD treatment. EDI achieved 95.3% water recovery and produced high-purity demineralized water with conductivity below 0.30 µS/cm. MD treatment of RO concentrate and ultra-concentrate achieved recoveries of 82% and 60%, respectively, producing permeate suitable for clarified water reuse. Additionally, MD permeate from RO concentrate showed adequate quality for further demineralized water production via EDI. EO treatment of MD concentrates reduced chemical oxygen demand (COD) to values below 30 mg/L, corresponding to removals greater than 63% and 91% for the RO concentrate-derived and ultra-concentrated RO-derived streams, respectively. Chloride removal reached 52.3% and 56.1%, respectively, although the removal of other inorganic constituents remained limited. Overall, the integrated system enabled 96 to 98% wastewater reuse, demonstrating strong potential for circular water management and zero liquid discharge strategies in petrochemical industries.

Check for updates

Received: 30 September 2026
Revised: 24 October 2026
Accepted: 29 October 2026
Published: 4 November 2026

Copyright: © 2026 by the authors. Licensee MDPI, Basel, Switzerland. This article is an open access article distributed under the terms and conditions of the Creative Commons Attribution (CC BY) license.

Keywords: petrochemical wastewater; water reuse; membrane separation process; electro-oxidation; zero liquid discharge

1. Introduction

Integrated refinery–petrochemical complexes produce a wide range of petroleum derivatives and petrochemical commodities. These processes are highly resource-intensive, consuming large amounts of water and energy and generating considerable waste and wastewater [1]. In response, circular economy strategies aim to improve resource efficiency, minimize waste generation, and reduce environmental impacts by promoting the reuse of resources across industrial operations [2]. These strategies also encourage the recovery and reuse of valuable resources from waste streams, as demonstrated in studies on soil-washing effluent treatment and resource recovery from stainless steel pickling wastewater [3,4]. Among these approaches, water reuse is particularly important for reducing freshwater withdrawals from natural sources [5,6]. However, direct reuse of petrochemical wastewater is hindered by the presence of complex contaminants, requiring advanced treatment to meet quality standards for reuse. In petrochemical facilities, different water qualities are required for specific operational purposes. Clarified water is used as fire water and for replenishing cooling systems and other processes, whereas demineralized water is essential for the safe generation of high-pressure steam. The latter must comply with stringent quality standards to prevent scaling and corrosion in boilers [7].

The urgency of developing high-efficiency water-reuse technologies is reinforced by global climate-change projections. South America has experienced severe droughts in the past and remains highly vulnerable to this phenomenon, with projections indicating increasing severity under future climate scenarios [8]. This growing pressure on major water users underscores the need to expand industrial water-reuse practices. For the petrochemical industry, which represents one of the largest industrial consumers of water in Brazil, these climatic shifts further reinforce the need for robust, flexible, and high-recovery treatment systems capable of reducing dependence on external water sources, transitioning toward closed-loop water-reuse schemes. Such approaches protect industrial productivity while preventing severe operational disruptions caused by water scarcity.

Membrane separation processes (MSPs) have been widely applied to remove recalcitrant organic compounds and dissolved salts from petrochemical wastewater [9–12]. Pressure-driven MSPs, such as microfiltration (MF), ultrafiltration (UF), nanofiltration (NF), and reverse osmosis (RO), are commonly employed. Electrodialysis (ED) and electrodeionization (EDI), MSPs using electric fields as the driving force [13], may also be applied. EDI has proven to be particularly effective for ion removal, and is frequently applied downstream of RO for the production of ultrapure water and make-up water in steam generation systems, as well as in pharmaceutical, semiconductor, and power industries [12]. Membrane distillation (MD), which operates based on a temperature gradient between the feed and permeate sides, has emerged as a promising alternative for treating high-salinity wastewater [14]. MD can operate at low temperatures and effectively handle concentrated waste streams such as RO concentrates (ROC), producing high-purity permeate with lower fouling susceptibility than pressure-driven processes [15], reducing the volume of concentrate discharged to the environment [16].

The performance of membrane-based processes varies with the technology and feedwater characteristics. In petrochemical wastewater treatment, integrated RO–EDR systems have achieved water recovery of 87.3% and chloride and alkalinity removal above 90% [9]. For MD, water recovery ranged from 56% to 75%, depending on pretreatment conditions [10],

while recovery close to 90%, and rejection above 99.5% for the parameters analyzed, were reported for RO concentrate treatment [17]. These findings highlight the potential of integrated treatment strategies to increase water recovery and reduce pollutant loads.

Despite their efficiency, MSPs generate concentrated waste streams. The ROC typically represents up to 50% of the RO feedwater [18–21], and its effective treatment remains a major challenge [22]. In many cases, this concentrate is discharged without adequate treatment, posing significant environmental risks [23]. Venzke et al. (2017) [24] demonstrated that the concentrate generated from a hybrid RO–EDR system treating petrochemical wastewater contained high levels of chloride, alkalinity, calcium, magnesium, sodium, and dissolved organic compounds, rendering it unsuitable for direct discharge.

To enhance water recovery and minimize waste generation, hybrid treatment systems that integrate advanced oxidation processes (AOPs) with MSPs have shown promising potential. AOPs rely on the generation of hydroxyl radicals (HO•), highly reactive species with a redox potential of 2.8 V, capable of degrading a wide range of organic pollutants [25–29]. Among the AOPs, electro-oxidation (EO) has emerged as an effective technology for treating MSP concentrates, particularly under high-salinity conditions [30]. EO generates strong oxidants, including hydroxyl radicals, reactive chlorine species (Cl•, ClO•), and sulfate radicals ($SO_4\bullet^-$), through salt-mediated electron transfer, enabling efficient degradation of residual organic matter [31]. Over the past two decades, EO has been extensively studied for ROC treatment using various anode materials, such as boron-doped diamond (BDD), Cu/Zn, Cu/Ni, Ti/TiO_2–RuO_2, Ti/PbO_2, Ti/SnO_2–Sb, Ti/RuO_2–Ir, and Ti_4O_7, with demonstrated effectiveness in removing chemical oxygen demand (COD), total nitrogen, and ammonium nitrogen [18,32,33].

Thus, this study proposes and evaluates a novel hybrid treatment system integrating UF, RO, EDI, MD, and EO to maximize water recovery and generate high-quality reuse water for petrochemical operations. The approach assesses the performance of each treatment step under progressively concentrated pollutant loads, enhances the valorization of membrane-process concentrates through complementary thermal and electrochemical treatments, and reduces the volume of the final waste stream. By advancing a more efficient pathway toward industrial zero-liquid-discharge (ZLD), this work contributes to strengthening climate-resilient water-management strategies, an increasingly critical need as refinery–petrochemical complexes face growing water scarcity and hydro-climatic variability driven by climate change. This research was conducted in a petrochemical complex in Brazil. This sector plays an important economic role both nationally and globally. The Brazilian chemical industry ranks sixth largest in the world, and the petrochemical sector represents approximately 20% of this industrial sector, with a net turnover of US$ 32 billion in 2025 [34].

2. Material and Methods

The wastewater used in this study was collected from the wastewater treatment plant (WWTP) of a petrochemical complex in southern Brazil, which generates an average of 706 m^3/h of wastewater. The conventional WWTP comprises preliminary treatment, including sand removal and oil–water separation, followed by an equalization tank and secondary treatment, using an activated sludge process with extended aeration and a secondary clarifier. After secondary treatment, the effluent undergoes tertiary polishing in a series of eight stabilization ponds before being discharged onto the soil. Wastewater samples for this study were collected from the final (eighth) stabilization pond at the following geographical coordinates: latitude −29.847130 and longitude −51.377370. The composition of the effluent treated by conventional WWTP is presented in Table 1. This effluent was then subjected to the additional treatment train evaluated in this study, as illustrated in Figure 1.

Table 1. Characterization of the treated petrochemical wastewater (conventional WWTP) used in the study.

Parameter	Conventional Treated Petrochemical Wastewater
Calcium (mg/L)	23.56
Chloride (mg/L)	136.96
Magnesium (mg/L)	7.520
Sulfate (mg/L)	304.00
Electrical conductivity (µS/cm)	1718.00
Iron (mg/L)	1.39
Chemical oxygen demand (COD) (mg/L)	58.60
Total suspended solids (TSS) (mg/L)	6.40
Turbidity (NTU)	52.97

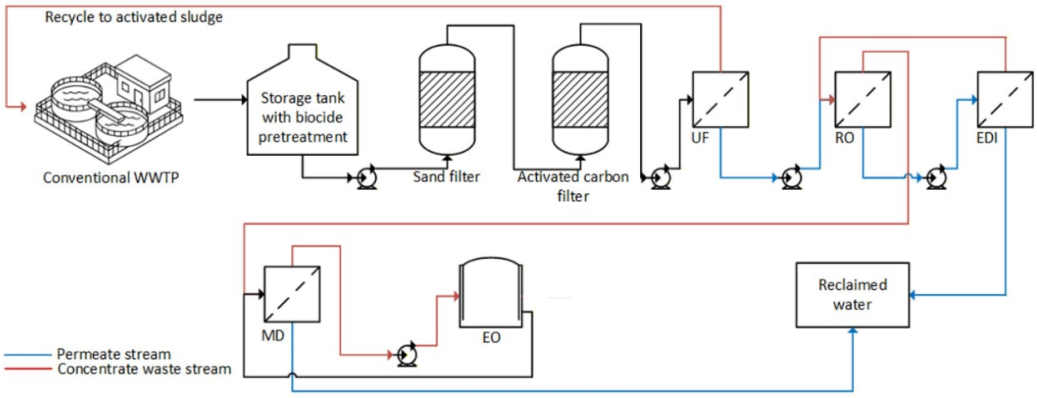

Figure 1. Flowchart of the proposed treatment of petrochemical wastewater for reuse.

In the petrochemical industry evaluated, two types of water are used (clarified and demineralized water) for distinct operational purposes. Clarified water, with a flow rate of 1298 m^3/h, is used as fire water, and to replenish the cooling water system and the coal boiler ash-handling system. Demineralized water, consumed at a flow rate of 389 m^3/h, must meet stringent quality standards to ensure the safe generation of high-pressure steam, preventing scaling and corrosion in boilers. This high-purity steam is critical for electricity production and serves as a heating medium in various industrial processes. The quality criteria for reclaimed water intended for use as clarified or demineralized water are summarized in Table 2 [7].

Table 2. Quality criteria for clarified and demineralized water in the evaluated petrochemical industry [7].

Parameter	Clarified Water	Demineralized Water
Aluminum (mg/L)	<0.5	ns
Conductivity (µs/cm)	165	<0.3
Iron (mg/L)	ns	<0.01
Magnesium (mg/L)	0.50	0.25
pH	7–8	6–7

ns: not specified.

2.1. Integrated UF/RO/EDI Treatment System

The integrated UF/RO/EDI treatment system consisted of sand and activated carbon filtration units, followed by UF, RO, and EDI. This treatment sequence was implemented in a pilot-scale water reuse unit, with a treatment capacity of 1 m^3/h (Figure 2). The wastewater

was pumped to two equalization tanks where 1 mg/L of the biocide Acticide® DB 20 (Thor, Wincham, UK) was dosed. The upflow filter consisted of three graded layers of sand (33 cm thick each, with 1.4, 0.9, and 0.4 mm particle size). The activated carbon bed (AlphaCarbo, Guarapuava, Brazil) was 1 m thick with 1 mm particle size. Post-filtration, 3.2 L/h of 0.7% sodium hypochlorite was dosed.



Figure 2. Pilot-scale reuse unit.

The UF system operated at 2.5 bar and 18 to 22 °C using a commercial polyvinylidene fluoride hollow fiber membrane (SFX-2860, Dow Water, Wilmington, DE, USA, 51 m^2). The RO system used a BW30 (4040) (Dow Water, Wilmington, DE, USA) polyamide membrane, operating at 5.0 bar with 50% recovery. The RO unit had an active membrane area of 7.2 m^2. The EDI system employed a commercial Ion Tech® (Beijing, China) ITDS 10 module comprising 10 cells packed with cationic and anionic ion exchange resins, 20 ion exchange membranes (0.044 m^2 each), totaling a membrane area of 0.88 m^2, and two electrodes (0.044 m^2 each). The cathode was made of stainless steel, and the anode was titanium coated with titanium dioxide. The current density of 34.1 A/m^2 was applied. The wastewater passed through a 20 µm disc filter before UF and a 5 µm disc filter before RO and EDI. The UF and RO tests were performed continuously for four weeks and the EDI test was performed continuously for 24 h.

The UF unit was cleaned every 30 min, consisting of a two-minute backwash with UF permeate, a one-minute air wash, a two-minute treatment with 0.7% sodium hypochlorite solution, and a final two-minute rinse with permeate. The RO unit was cleaned daily for five minutes with permeate. The EDI system was cleaned prior the 24-h test by 30 min recirculating 5% sodium chloride solution, followed by a 30-min treatment with 1% sodium hydroxide solution and a three-minute rinse with RO permeate. In the second stage, sanitization was performed with 1% sodium percarbonate for 30 min, followed by a 5% sodium chloride rinse and a three-minute permeate rinse. The third stage involved recirculation of 2% hydrochloric acid for 30 min, rinsing with 5% sodium chloride solution, and a final three-minute rinse with RO permeate.

2.2. Treatment of RO Concentrate (ROC) and Ultra-Concentrated (ROUC) Waste Streams Using MD

The ROC was treated using a laboratory-scale Direct Contact Membrane Distillation unit (Figure 3). To assess MD performance with more concentrated feeds, the ROC was further concentrated by recirculating it through the RO system once, under the same operating conditions (50% recovery and 5 bar pressure) resulting in a RO ultra-concentrated waste stream (ROUC). Pre-concentration using RO has been previously reported as an effective strategy to minimize concentrate waste generation [35,36].

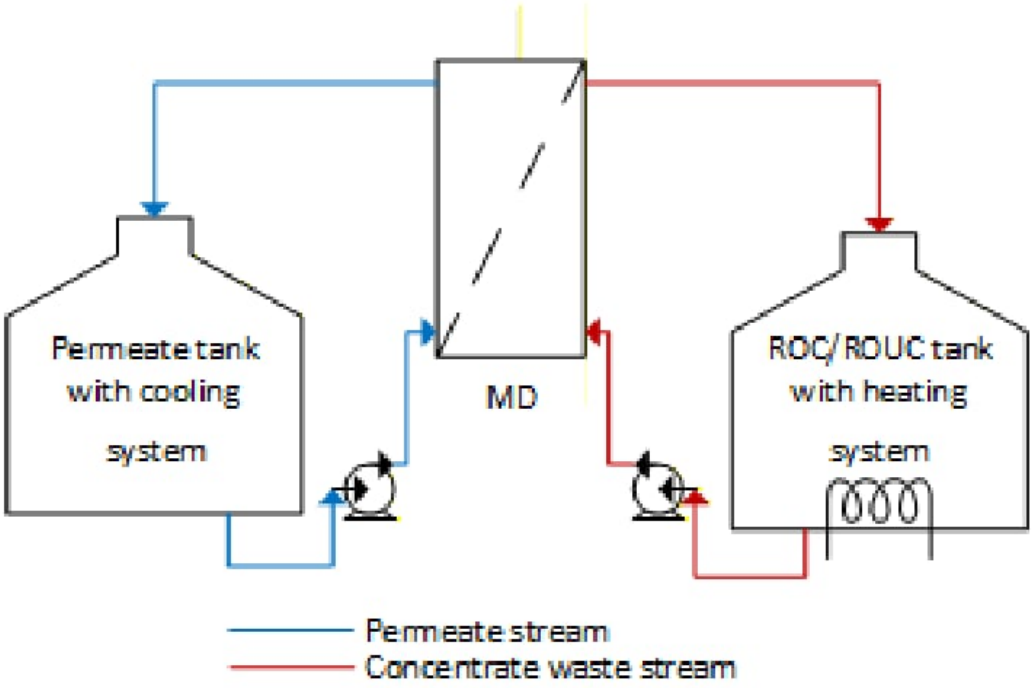

Figure 3. Schematic representation of the laboratory-scale MD unit.

The MD unit had an adjustable processing capacity ranging from 40 to 170 L/h. It comprised a 30 L feed tank equipped with a 3 kW electric heating coil and a 25.4 L permeate tank. The membrane module and spacer were made of polypropylene, providing an effective membrane surface area of 0.023 m^2. Microporous, flat-sheet polyethylene membranes (Aquastill, Sittard, The Netherlands) were employed. For the ROC experiment, the membrane had a pore size of 0.3 µm, porosity of 80%, and a contact angle above 118°. For the ROUC experiment, the membrane had a pore size of 0.2 µm, porosity of 85%, and a contact angle of 60°.

Both ROC and permeate were circulated at a flow rate of 84 L/h. The ROC temperature was maintained at 60 °C, while the permeate was kept at 20 °C. The system operated in full recirculation mode. The MD test with ROC was conducted for 1080 h, and the ROUC tests were performed under identical conditions for 480 h. When a flux drop was observed, membrane cleaning was performed by flushing with 30 L of deionized water at 60 °C and a tangential velocity of 0.02 m/s, followed by chemical cleaning with 2% hydrochloric acid, and mechanical cleaning using a soft sponge.

2.3. Treatment of MD Concentrate Waste Stream Using EO

The concentrated waste streams produced by the MD process using ROC (MDC) and ROUC (MDUC) were treated using a laboratory-scale EO system (Figure 4). The setup comprised a 2 L feed tank, a pump (Seaflo, SFDP1-040-060-51, Xiamen, China), and a recirculation valve to recycle excess flow. The inlet flow to the electrode module was fixed at 75 L/h. A DC power supply (Icel, Manaus, Brazil, PS 6000 0–32 V, 0–6 A) provided the applied currents, with voltage monitored and adjusted during operation. The EO module was constructed from acrylic material and equipped with dimensionally stable anode (DSA®), flat-plate electrodes composed of Ti/TiO_2 (70%) and RuO_2 (30%), each with an active area of 100 cm^2 (10 cm × 10 cm). Current densities of 20, 30, and 40 mA/cm^2 were tested for MDC, and current densities of 30, 40, and 50 mA/cm^2 were tested for MDUC. The pH was monitored hourly throughout each 5-h electro-oxidation experiment, along with the applied voltage. No pH adjustment procedure was performed during these experiments.

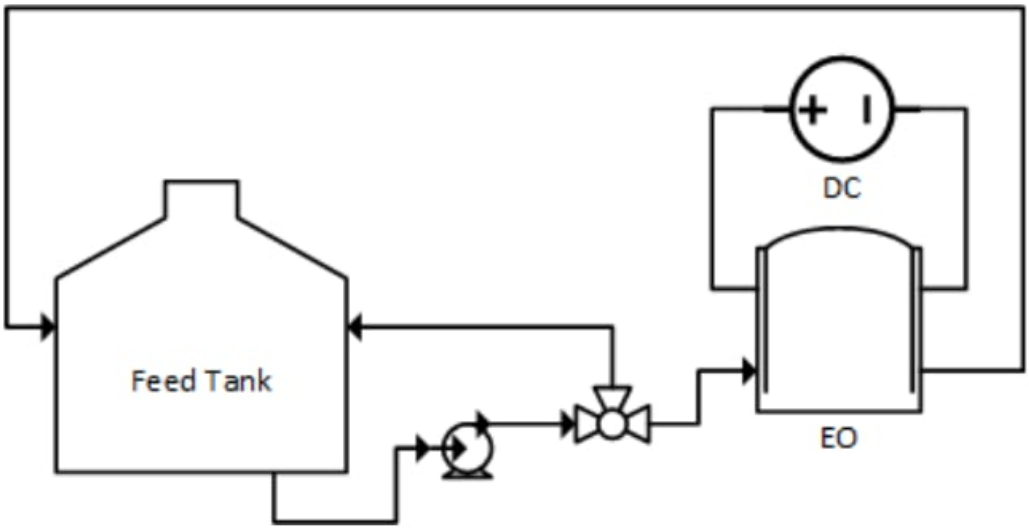

Figure 4. Schematic representation of the EO system, including the feed tank, pump, recirculation valve, DC power supply, and acrylic module with electrodes.

2.4. Physicochemical Characterization of Aqueous Streams

The parameters used to characterize the permeate and concentrate waste streams from the MSPs and EO wastewater, along with their respective analytical methods, are presented in Table 3.

Table 3. Physicochemical parameters and analytical methods for aqueous stream characterization.

Parameter	Analytical Method	Analyzed Stream
Calcium	[31]	MSP, EO
Chloride	[37]	MSP, EO
COD	[38]	MSP, EO
Electrical conductivity	[39]	MSP, EO
Iron	[40]	MSP
Magnesium	[40]	MSP, EO
pH	[41]	MSP, EO
Potassium	[42]	EO
Sodium	[43]	EO
Sulfate	[37]	MSP, EO
Total solids	[44]	EO
Turbidity	[45]	MSP
TSS	[46]	MSP

2.5. Characterization of EDI and MD Membranes, Ion Exchange Resins, and EO Electrodes

Surface morphology was analyzed using a JEOL JSM 6010LA SEM. Images were acquired in secondary electron imaging mode under high vacuum, at an accelerating voltage of 10 kV and a working distance of 10 mm. Magnification was adjusted according to the sample characteristics. Elemental composition was determined by EDS using the SEM-EDS system operated at 10 kV with a working distance of 12 mm. Micrographs were acquired for the cation and anion-exchange membranes of the EDI unit, the ion-exchange resins from the dilute and concentrate compartments, and the MD membranes used with ROC and ROUC feeds.

Thermogravimetric analyses of the EDI and MD membranes and EDI resins were performed in accordance with the ASTM E1131:2020 standard [47]. The analyzes were conducted using a TA Instruments TGA Discovery system, with a heating rate of 10 °C/min

under a nitrogen atmosphere. A Platinum HT crucible and an Evolved Gas Analysis oven were employed, with a nitrogen flow rate of 25 mL/min.

The hydrophobicity of the MD membranes was evaluated in their pristine state, and after ROC/ROUC treatment and cleaning. Contact angles were measured using ultrapure water on membrane samples (2 × 4 cm) cut from both pristine and post-cleaning membranes. Prior to analysis, the samples were air-dried under ambient conditions. Measurements were performed using the sessile drop method with a goniometer (Phoenix Mini), applying 1.8–2.0 µL of ultrapure water to the membrane surface. For each sample, five measurements were taken at different positions, and the average value was reported as the contact angle.

The electrodes used in the EO tests were analyzed by X-ray fluorescence spectrometry to determine their elemental composition. Measurements were performed using a Thermo Scientific Niton XL3t GOLDD+ analyzer. Each electrode was exposed to the instrument's X-ray source, allowing qualitative and quantitative identification of the constituent elements. The acquisition time was 94 s for the anode and 90 s for the cathode.

2.6. Water Balance of Hybrid Wastewater Treatment Processes

A water balance was developed considering the average flow rate of wastewater treated at the conventional petrochemical WWTP. The analysis was based on the recovery rate of each treatment process, defined as the ratio of permeate produced to feed supplied, in order to quantify the fraction of wastewater that could be effectively reused. This approach enabled the estimation of the total volume of wastewater currently discharged by the industry that could be redirected for reuse through the proposed hybrid treatment system. The balance was carried out considering the two treatment possibilities, using ROC and ROUC.

3. Results and Discussion

3.1. Operational Stability and Performance of Membrane Separation Processes

Figure 5 shows the evolution of permeate flux and turbidity for UF (a), permeate flux and electrical conductivity for RO (b), EDI (c), and MD using ROC (d) and ROUC (e). The applied voltage is also shown for EDI (c).

The UF system achieved 91.5% water recovery with an average flux of 19 L/h·m^2 (Figure 5a). The average pressure at the UF module inlet was 1.7 bar. The flux remained stable throughout the four-week testing period, which can be attributed to the frequent membrane cleanings, performed every 30 min. A previous study [48] on UF treatment of petrochemical wastewater attributed membrane fouling mainly to physical interactions (particle deposition driven by hydrodynamic pressure) and recommended a 3-min backwash every hour of operation, a strategy comparable to the procedure applied in this study.

The RO system achieved 50.5% water recovery with an average flux of 21 L/h·m^2 (Figure 5b). The average pressure at the RO module inlet was 4.8 bar. The addition of biocides likely contributed to controlling microbial proliferation, thereby maintaining the stability of the RO permeate flow, as also observed in a previous study [11]. The low flux variation suggests that UF pretreatment ensured sufficient feedwater quality for RO operation, minimizing membrane fouling, results consistent with those reported for petrochemical wastewater treatment [49].

Throughout the evaluation period, the RO permeate conductivity remained below 30 µS/cm, meeting the quality criteria for EDI feedwater (<40 µS/cm) [50]. The small variations observed in conductivity were attributed to the natural variability of the feedwater composition, a typical feature of real wastewater streams such as the tertiary petrochemical effluent used in this study. The RO system also operated at reduced pressure (<6 bar) due to the low osmotic driving force of the feedwater [51], while still producing permeate of adequate quality for subsequent electrodeionization.

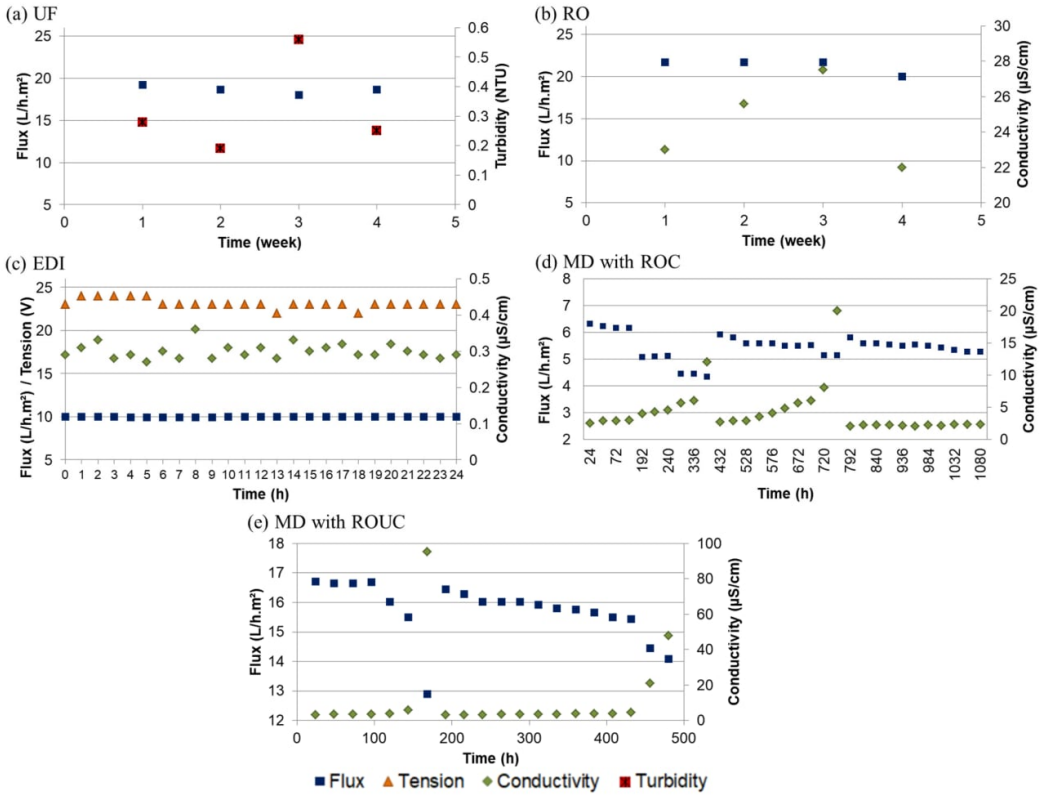

Figure 5. Evolution of permeate flux and permeate parameters (turbidity and conductivity) over the time of operation of the following units: UF (**a**), RO (**b**), EDI (**c**), and MD with ROC as feed (**d**), and MD with ROUC as feed (**e**). EDI also includes the applied tension.

The EDI system operated continuously for 24 h, achieving 95.3% water recovery and an EDI diluted flux of 10 L/h·m^2 (Figure 5c). The resulting EDI diluted stream exhibited an electrical conductivity of 0.3 µS/cm and a pH of 6.45, meeting the specifications of high-purity demineralized water conductivity below 0.3 µS/cm and pH 6.0 to 7.0 (Table 2). Due to the stringent feedwater quality requirements of EDI systems, various pretreatment strategies have been investigated when wastewater is used as the source. For potable water, pretreatment often involves two RO stages [52]. When wastewater is used as feedwater, integrated pretreatment processes such as UF/RO are required to meet the quality demands of EDI [13]. In this study, wastewater with an initial conductivity of 1700 µS/cm was successfully treated by UF and RO, producing high-quality permeate to feed the EDI system.

The MD system operated for 1080 h with ROC feed, achieving 82% water recovery and an average permeate flux of 5.6 L/h·m^2 (Figure 5d). A gradual increase in permeate conductivity and decrease in permeate flux were observed over time, likely due to membrane wetting. Fouling contributes to reduced membrane hydrophobicity, which promotes pore wetting, flux decline, and conductivity rise, particularly during long-term operation when the membrane surface becomes more vulnerable to fouling and scaling [53,54]. At 360 h, when the permeate conductivity reached 12 µS/cm (Figure 5d), operation was interrupted for membrane cleaning. A second cleaning was performed at 744 h, after conductivity reached 20 µS/cm. Similar trends of conductivity rise and flux reduction have been reported in the literature [53] with stable operation for approximately 100 h using PE membranes, underscoring the extended operational stability achieved in this study.

The MD system operated for 480 h using the ROUC feed, achieving 60% water recovery and an average permeate flux of 15.4 L/h.m^2 (Figure 5e). The higher permeate flux observed for the ROUC membrane may be associated with differences in membrane properties and feed composition. However, the substantial difference in water contact angle between the

ROC and ROUC membranes (118° and 60°, respectively) limits direct comparisons of their flux and anti-wetting performance. Therefore, the individual contributions of membrane porosity, surface wettability, and feed characteristics to the observed flux differences cannot be clearly distinguished under the experimental conditions investigated. The ROUC test duration was shorter compared to the ROC, as the ROUC feed was more concentrated. The first cleaning was performed after 144 h of operation due to an increase in permeate conductivity, which reached 95.10 µS/cm. Cleaning restored the initial conductivity level; however, after 432 h of operation, new permeate contamination was observed. Thus, the more concentrated ROUC feed, compared to the ROC, tends to require more frequent cleaning, which may lead to a reduction in the MD membrane's operational lifetime.

3.2. Characterization of Permeate from Membrane Separation Processes

Figure 6 presents the characterization of the permeate streams from all treatment stages using membrane separation processes, showing the results for calcium (a), chloride (b), magnesium (c), sulfate (d), conductivity (e), iron (f), COD (g), total suspended solids (h), and turbidity (i).

The petrochemical wastewater used as feed in this study contained 23.56 mg/L calcium (Figure 6a), 136.96 mg/L chloride (Figure 6b), 7.520 mg/L magnesium (Figure 6c), and 304.0 mg/L sulfate (Figure 6d). After UF, these ionic species showed slight reductions, except for chloride, which exhibited a minor increase, possibly due to the biocide dosage. Substantial reductions (>90%) were achieved following RO, particularly for ions that pose a risk of scaling in the EDI system [55]. The EDI stage provided additional removal of chloride and magnesium, while calcium and sulfate were already below the quantification limit after RO (0.50 mg/L for both calcium and magnesium). The effective removal of calcium and magnesium is noteworthy, as these ions are primary contributors to scaling and corrosion in steam generation systems [56]. Magnesium concentrations in the final effluent met the reuse standard for demineralized water (<0.25 mg/L; Table 2).

Conductivity followed a similar trend (Figure 6e), the high values observed in the petrochemical wastewater (1718 µS/cm) and UF permeate (1622 µS/cm) were reduced to 10.73 µS/cm after RO, providing a high-quality feed for EDI and preventing fouling of spacer channels and resin degradation [57]. The EDI effluent achieved a conductivity below 0.30 µS/cm, meeting the standard for reuse as demineralized water (Table 2).

Iron (Figure 6f), present at 1.39 mg/L in the petrochemical wastewater was removed by 92% during UF, consistent with previous findings on the effectiveness of UF for iron removal [58]. Subsequent removal by RO and EDI could not be quantified, as iron was already below the quantification limit (0.10 mg/L) after UF. COD (Figure 6g) was primarily reduced during RO, while total suspended solids (Figure 6h) and turbidity (Figure 6i) were effectively removed in the UF step. These results highlight the complementary roles of each technology in the integrated UF/RO/EDI system for demineralized water production. Comparable results were reported by Katsoyiannis et al. (2017) [59], who achieved removals of chloride (98%), sodium (99%), potassium (65%), magnesium (100%), and calcium (89%) using ion-exchange resins in separate and mixed-bed configurations. Nevertheless, EDI presents a clear advantage over conventional ion exchange, as it eliminates the need for chemical regenerants, allowing continuous operation and reducing environmental impacts.

MD was applied to the ROC and ROUC streams to enhance water recovery for water reuse. Both ROC and ROUC exhibited high conductivity and elevated concentrations of chloride, sulfate, and COD (Table 4), consistent with values reported by Santos et al. (2020) [10] and Venzke et al. (2021) [17] for petrochemical wastewater. In contrast, the MD permeate presented low concentrations for all evaluated parameters, with removal efficiencies exceeding 90%, corroborating previous MD performance results (91–99%)

reported by Venzke et al. (2021) [17]. The exception was COD for ROUC treatment, due to the quantification limit of the analysis (30 mg/L).

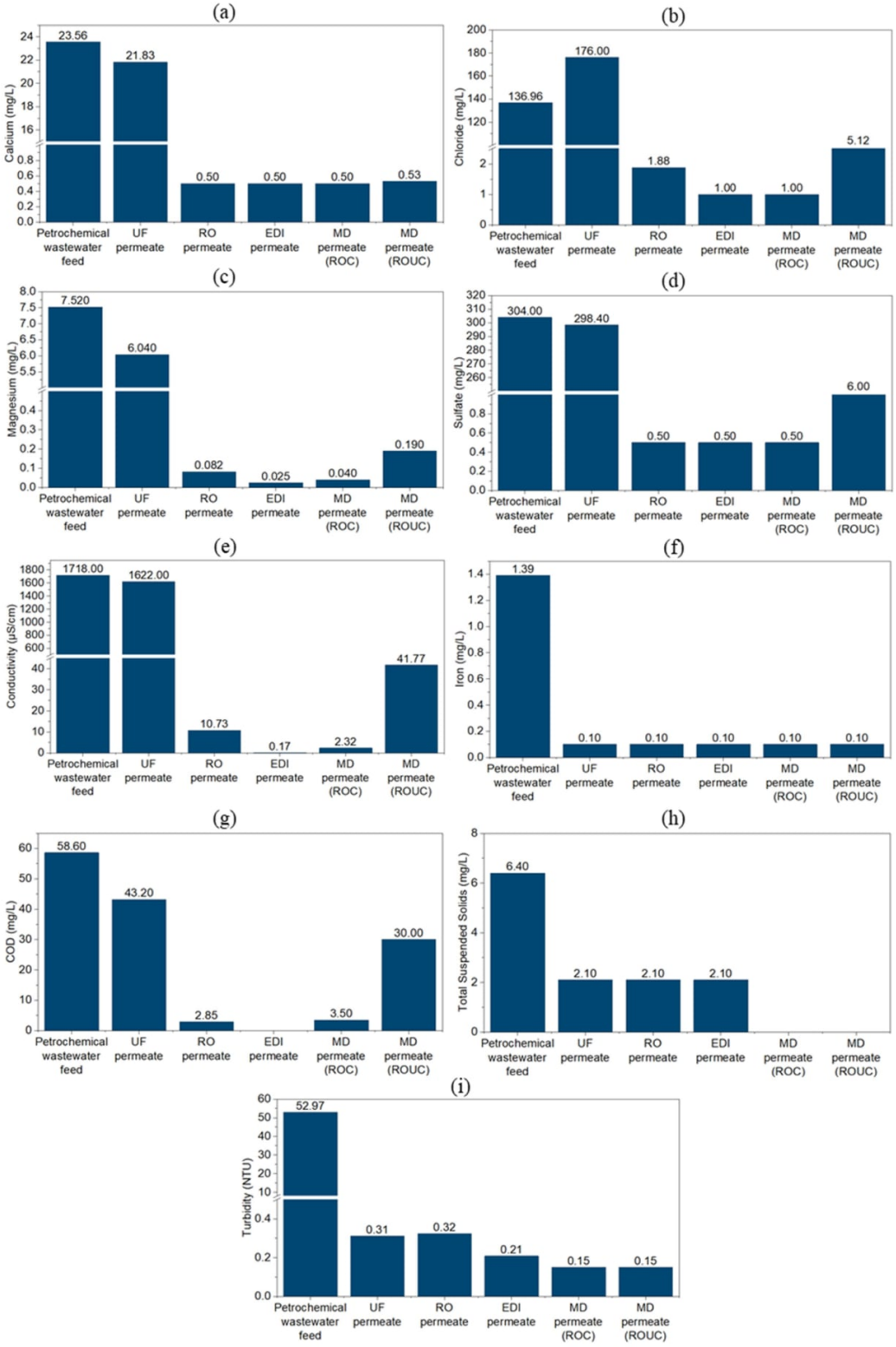

Figure 6. Content of specific elements and some parameters of the feed and the permeate from all membrane treatment stages: calcium (**a**), chloride (**b**), magnesium (**c**), sulfate (**d**), conductivity (**e**), iron (**f**), COD (**g**), total suspended solids (**h**), and turbidity (**i**) in permeate streams.

Table 4. Physicochemical characterization of ROC and ROUC feed streams and their corresponding MD permeates, with assessment of MD process efficiency.

Parameter	ROC	MD Permeate (from ROC)	Efficiency	ROUC	MD Permeate (from ROUC)	Efficiency
Calcium (mg/L)	42.12	<0.50	>98.81%	157.10	0.53	99.66%
Chloride (mg/L)	301.39	<1	>99.67%	844.37	5.12	99.39%
Magnesium (mg/L)	17.00	<0.04	>99.72%	44.20	0.19	99.56%
Sulfate (mg/L)	478.61	<0.50	>99.90%	1316.31	6.00	99.54%
Electrical conductivity (µS/cm)	2579.33	2.32	99.91%	6350.00	41.77	99.39%
Iron (mg/L)	<0.10	<0.10	-	<0.10	<0.10	-
COD (mg/L)	59.23	<3.50	>90.35%	59.76	<30	>49.80%
Total suspended solids (mg/L)	<15.00	<15.00	-	<15.00	<15.00	-
Turbidity (NTU)	1.64	0.15	90.89%	0.15	0.15	-

Although the MD permeates from both ROC and ROUC did not meet the conductivity requirement for demineralized water (Figure 6e), they complied with the clarified water limit (<165 µS/cm) (Table 2), making them suitable for reuse in production, cooling, and firefighting systems [7]. The MD permeate obtained from ROC exhibited quality comparable to or even superior to that of the RO permeate (Figure 6) for most parameters, with only a slightly higher COD (3.50 mg/L for MD vs. 2.85 mg/L for RO), confirming its feasibility as EDI feedwater for demineralized water production. In contrast, the MD permeate derived from ROUC showed higher concentrations of chlorides, magnesium, sulfates, and COD (Table 4), as well as greater conductivity compared to the RO permeate, suggesting an increased potential for fouling in the EDI system. The conductivity of the MD permeates from ROUC (41.77 µS/cm) also exceeded the recommended limit for EDI feedwater (<40 µS/cm) [50].

3.3. Treatment of MD Concentrate Waste Stream Using EO

Figure 7 shows the COD removal from MDC (a) and MDUC (b) after 3 and 5 h of EO treatment. For both wastewaters, COD values below the quantification limit (30 mg/L) were achieved at higher current densities. After 5 h of operation, COD was below the quantification limit at 30 and 40 mA/cm^2 for MDC and at 40 and 50 mA/cm^2 for MDUC, corresponding to COD removals greater than 63% and 91%, respectively. Current density was identified as the primary parameter governing the EO reaction rate. Similar behavior has been reported in previous studies [31,60], which observed a linear decrease in COD with increasing current density due to the enhanced generation of hydroxyl radicals and active chlorine species (formed from chloride salts in the concentrate), the main oxidants in the system. However, extending EO treatment beyond 5 h generally does not result in additional COD reduction. Previous studies of Silva et al., (2019) [60] and Chen et al., (2022) [31] reported that COD removal plateaus after this period, even at higher current densities. This is attributed to a decline in current efficiency at elevated current densities, as mass transfer rather than electrical current becomes the limiting factor [61].

Table 5 summarizes the results of the parameters evaluated after 5 h of electro-oxidation (EO) under different current densities.

Increasing the current density enhanced chloride removal for both MDC and MDUC (Table 5), likely due to the oxidation of chloride ions into chlorinated oxidants that promoted organic matter degradation (Figure 7). At 40 mA/cm^2, the chloride concentration in MDC decreased from 1133.94 to 541.31 mg/L (52.3% removal), while at 50 mA/cm^2, the chloride

concentration in MDUC decreased from 1845.12 to 810.78 mg/L (56.1% removal), consistent with previously reported values [31]. Zhao et al. (2024) [62] demonstrated that chloride ions at the anode surface significantly improve hydroxyl radical conversion efficiency, favoring the formation of secondary oxidants such as active chlorine, which accelerate organic matter degradation, achieving COD removals of up to 94.5% at 20 mA/cm^2.

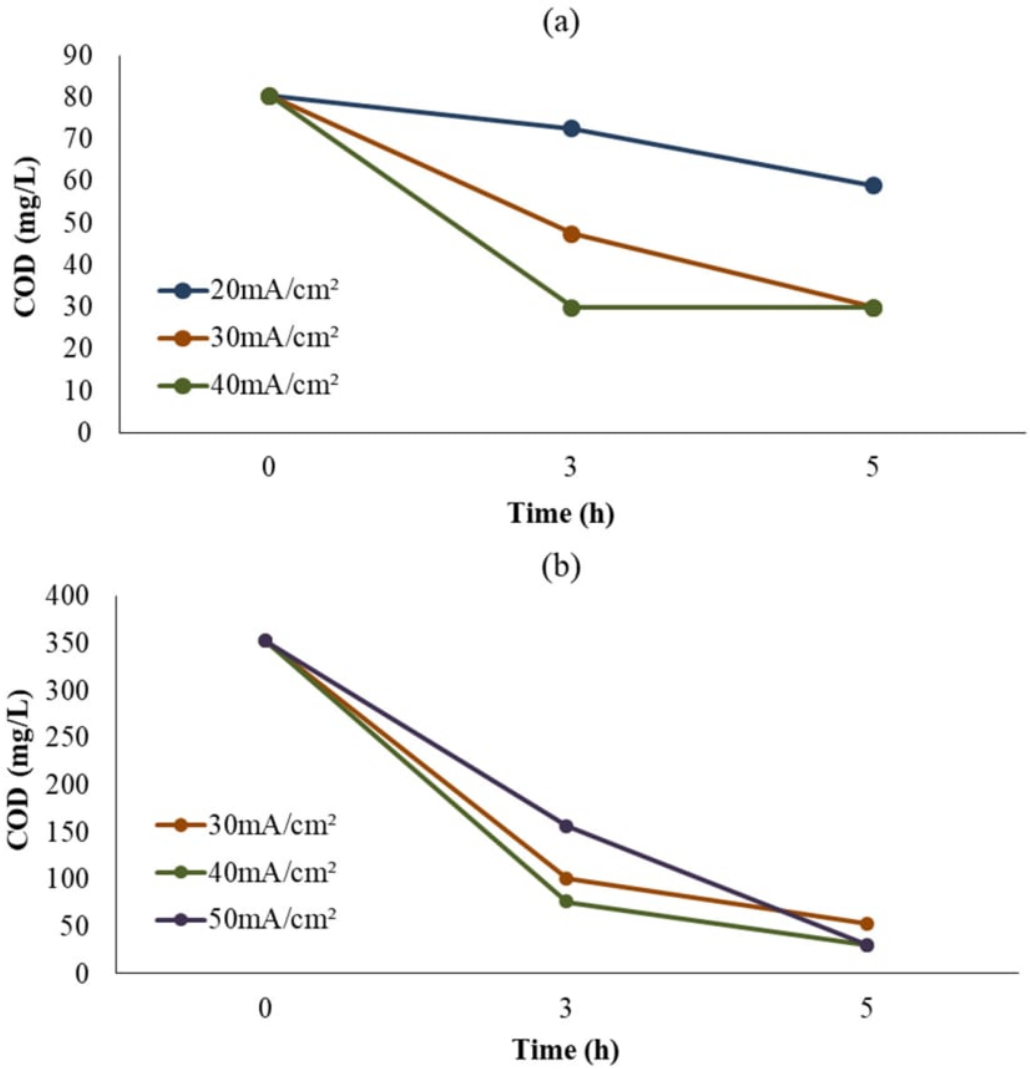

Figure 7. Behavior of COD removal from MDC (**a**) and MDUC (**b**) over the 5 h of EO operation.

The initial pH values of MDC and MDUC were alkaline (8.88 for both) and decreased progressively over time at all applied current densities. The lowest final pH was 8.36 for MDC at 30 mA/cm^2 and 8.53 for MDUC at 50 mA/cm^2. This pH decrease is attributed to several processes occurring at the dimensionally stable anode: (i) H^+ generation during water oxidation, (ii) formation of acidic oxidizing species such as hypochlorous acid (HOCl) from chloride oxidation, and (iii) production of acidic byproducts from the oxidation of organic compounds, including carboxylic acids and intermediates that release protons during degradation [63].

For parameters directly affecting the MD process and related to membrane scaling (potassium, sodium, and sulfate), removal efficiencies remained below 10% for MDC and below 30% for MDUC across all current densities (Table 5). Magnesium exhibited the highest removal for MDC at 30 mA/cm^2 (36.6%) and for MDUC at 50 mA/cm^2 (64.9%), while calcium removal from MDC was approximately 20% under all conditions and ranged

from 14.7% to 26.6% for MDUC (Table 5). Salt precipitation on the electrode surface can occur during EO depending on operating conditions and electrolyte composition. Several mechanisms are involved: (i) reactions between ions and oxidizing species (e.g., HO•, active chlorine) that may form insoluble compounds [64,65]; (ii) local supersaturation near the anode surface due to elevated ion concentrations and pH gradients; and (iii) scaling, where high salt concentrations lead to precipitation of carbonates, sulfates, or chlorides, forming a deposit layer on the electrode. This scaling reduces electrochemical efficiency by obstructing active anode sites [63].

Table 5. Characterization of MDC and MDUC before and after 5 h of EO at different current densities.

Parameter	Raw MDC	Treated MDC			Max. Efficiency (%)	Raw MDUC	Treated MDUC			Max. Efficiency (%)
		20 mA/cm^2	30 mA/cm^2	40 mA/cm^2			30 mA/cm^2	40 mA/cm^2	50 mA/cm^2	
Calcium (mg/L)	64.15	50.32	50.82	51.17	21.6	43.00	36.67	32.67	31.58	26.6
Chloride (mg/L)	1133.94	732.41	710.14	541.31	52.3	1845.12	1289.04	968.15	810.78	56.1
Conductivity (µS/cm)	6750	5700	5760	5600	17.0	11,510	8937	8180	8490	28.9
Magnesium (mg/L)	7.40	6.93	4.69	6.98	36.6	6.16	3.655	3.310	2.165	64.9
pH	8.88	8.47	8.36	8.50	-	8.88	8.62	8.54	8.53	-
Potassium (mg/L)	575.00	556.25	555.00	535.00	7.0	985.0	855.0	732.5	822.5	25.6
Sodium (mg/L)	1455.00	1360	1355	1340	7.9	2445.0	2005.0	1730.0	1937.5	29.2
Sulfate (mg/L)	2002.15	1852.74	1855.79	1835.69	8.3	2994.96	2572.97	2147.31	2568.14	28.3
Total solids (mg/L)	5540	5468	5576	5543	1.3	8686.0	7901	7033	7968	19.0

MDC treated at 40 mA/cm^2 (Table 5) exhibited calcium concentrations comparable to the initial ROC (42.12 mg/L) and lower magnesium levels (17.00 mg/L), indicating that EO treatment enhanced MDC's suitability as MD feed. Nevertheless, conductivity, chloride, potassium, sodium, and sulfate levels of MDC (Table 5) remained higher than those in the ROC (2579.33 µS/cm, 301.39 mg/L, 151.50 mg/L, 365.00 mg/L, and 478.61 mg/L, respectively). Similarly, MDUC treated at 50 mA/cm^2 (Table 5) showed lower calcium and magnesium concentrations than the ROUC (157.05 mg/L and 44.20 mg/L, respectively), while chloride levels were comparable (844.37 mg/L for ROUC). This suggests that EO treatment improved MDUC quality and its potential as MD feed. However, conductivity, potassium, sodium, and sulfate concentrations of MDUC (Table 5) remained elevated relative to ROUC (>5000.00 µS/cm, 467.00 mg/L, 1005.00 mg/L, and 1316.31 mg/L, respectively). Overall, EO treatment effectively reduced COD and chloride concentrations in both MDC and MDUC, but its impact on other inorganic constituents was limited, indicating that additional post-treatment steps may be necessary to ensure the long-term reuse of EO-treated effluents as MD feed. In addition, current efficiency, energy consumption, electrode lifetime, and potential byproduct formation were not assessed and warrant further investigation.

3.4. Characterization of EDI and MD Membranes, Ion Exchange Resins, and EO Electrodes

Figure 8 presents the SEM and EDS analyses for anionic (a,b) and cationic (c,d) EDI membranes after treatment of petrochemical wastewater. Both the anionic (Figure 8a) and cationic (Figure 8c) membranes exhibited similar morphological characteristics, showing a homogeneous polymeric structure. No surface deposits were observed, likely due to the effectiveness of the cleaning procedures applied during the experiments. EDS spectra revealed the presence of elements characteristic of the polymeric matrix and functional groups of the membranes: C, O, and Cl for the anionic membrane (Figure 8b), and C, O, S,

Na, and Cl for the cationic membrane (Figure 8d). Elements commonly associated with fouling (such as Ca, Fe, P, Mg, and K) were not detected, despite being present in the feed effluent of the electrodeionization system. This confirms the effectiveness of the chemical cleaning process.

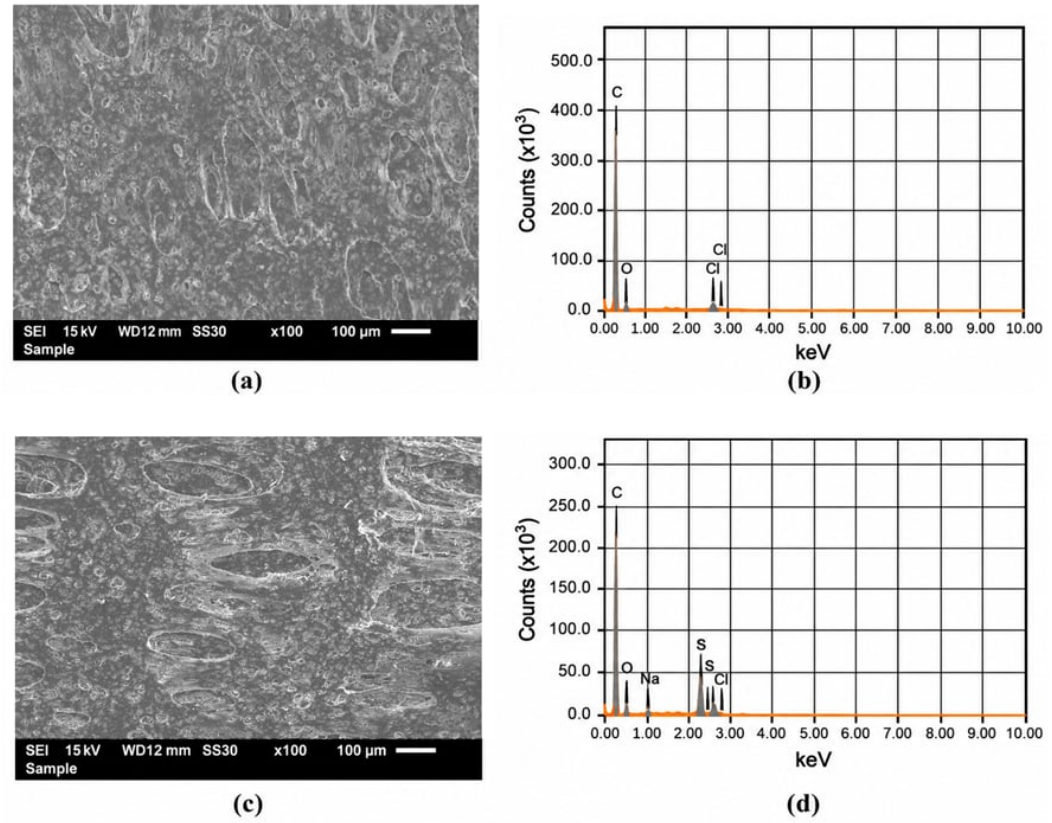

Figure 8. SEM and EDS analyses for anionic (**a**,**b**) and cationic (**c**,**d**) EDI membranes after treatment with petrochemical effluent.

Figure 9 presents the SEM and EDS analysis for ion-exchange resins from the concentrate (a,b) and dilute (c,d) compartments. The resins removed from the concentrate compartment of the EDI module retained their spherical morphology and structural integrity (Figure 9a). It was observed some material adhered to their surface. Figure 9c shows that the resins from the dilute compartment exhibited smaller amounts of surface deposits compared to those from the concentrate compartment. The EDS spectra (Figure 9b,d) indicate the presence of the characteristic elements of the resin matrix (C, O, Cl, and S).

Figure 10 presents the SEM and EDS analyses for MD membranes pristine (a,b), after use with ROC and cleaning (c,d), and after use with ROUC and cleaning (e,f). After chemical cleaning of the MD membranes (Figure 10c,e), surface deposits were still observed compared to the pristine membrane (Figure 10a), with more pronounced accumulation on the ROUC membrane, likely due to the higher salinity of the ROUC. The EDS spectrum of the pristine membrane (Figure 10b) revealed only carbon and oxygen, the characteristic elements of the membrane material. Following the treatment of ROC and ROUC wastewater (Figure 10d,f), and despite cleaning with 2% of hydrochloric acid, EDS analysis revealed the presence of deposited elements such as Si, Mg, and Ca, ions typically associated with inorganic fouling and the consequent flux decline [66], as well as Na and Zn.

Thermogravimetric analysis was conducted to assess the thermal properties and stability of the membranes and resins. This technique enabled the determination of decomposition temperatures, thermal degradation behavior, and overall material stability of the EDI and

MD membranes and EDI resins. Figure 11 presents the mass loss curve (a) and the derived weight (b) for the anionic and cationic EDI membranes.

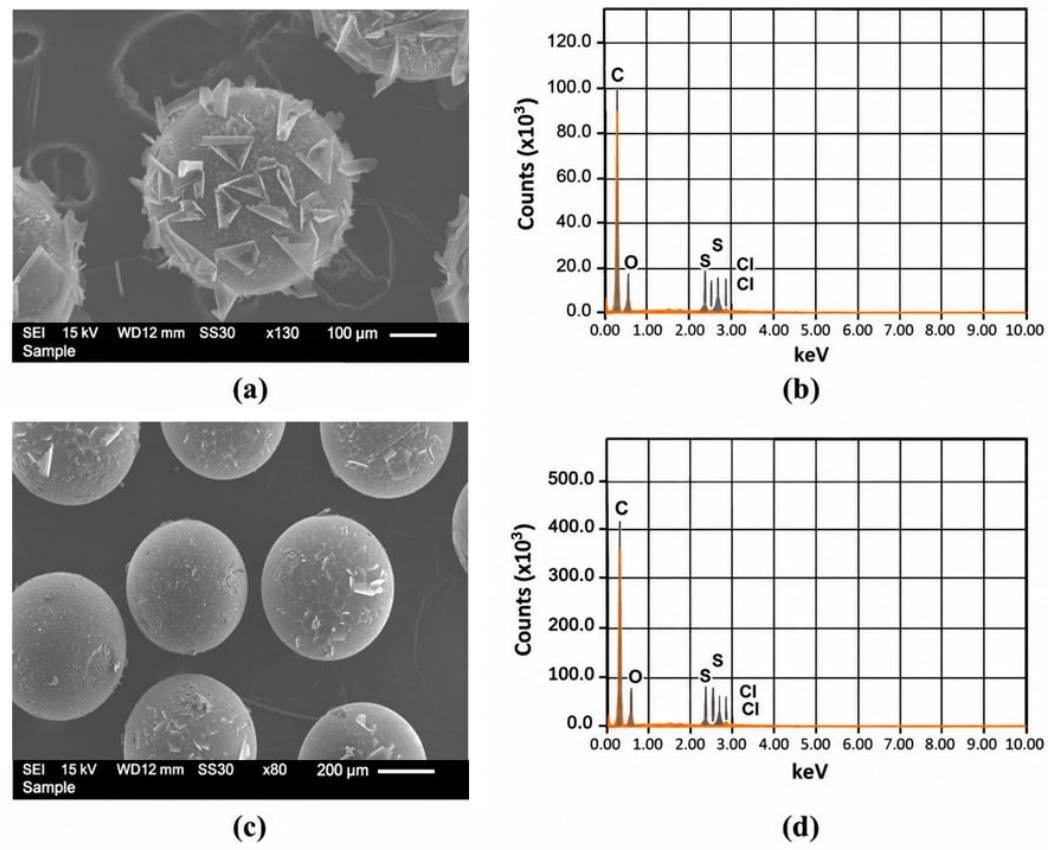

Figure 9. SEM and EDS analyses for ion-exchange resins from the concentrate (**a**,**b**) and dilute (**c**,**d**) compartments.

The thermogravimetric analysis of the EDI anion membrane (amino-functionalized polypropylene) (Figure 11) revealed notable differences compared to unmodified polypropylene, due to the incorporation of amino groups that modify the material's thermal stability and decomposition profile. An initial mass loss was observed up to 200 °C, corresponding to the release of adsorbed water or residual volatile solvents. The decomposition of amino groups occurred at approximately 246 °C, marking the onset of mass loss. Degradation of the polypropylene main chain was observed at around 479 °C, consistent with the typical decomposition range of pure polypropylene (350–500 °C). For the EDI cation membrane (Figure 11), thermal decomposition began at 368 °C, associated with the presence of sulfonic groups. These functional groups introduced an additional decomposition phase compared to pure polypropylene. In this temperature range, the sulfonate groups underwent thermal degradation, resulting in a significant mass loss of 68.86%.

Figure 12 presents the mass loss curve (a) and the derived weight (b) for the concentrate and dilute compartments resins.

Differences in the thermogravimetric profiles of the resins from the concentrated and diluted compartments reflect the distinct functional groups attached to their polystyrene–divinylbenzene matrices. The TGA of the resin from the concentrate compartment (Figure 12) (polystyrene-divinylbenzene functionalized with quaternary ammonium groups, R_4N^+) reveals characteristic thermal decomposition behavior of anion exchange resins. The functionalization influences both the thermal stability and decomposition profile of the material. An initial mass loss of 36.61% was observed between 50 °C and 150 °C, associated with the removal of adsorbed and hydration water, given the strong moisture affinity

of quaternary ammonium groups. Decomposition of these thermally unstable quaternary ammonium groups occurred between 200 °C and 350 °C, releasing volatile products such as amines and ammonia and resulting in an additional 11.10% mass loss. The degradation of the polystyrene-divinylbenzene matrix commenced at approximately 413 °C. For the resin from the dilute compartment (Figure 12) (polystyrene-divinylbenzene functionalized with sulfonic acid groups, $–SO_3H$), the first stage of mass loss (50–150 °C) corresponded to the release of bound water, attributed to the high hygroscopicity of sulfonate groups. Thermal degradation of these sulfonate groups occurred between 200 °C and 300 °C, with a mass loss of 11.44% due to the elimination of functional groups. Decomposition of the main polymer matrix began at around 410 °C, accompanied by a mass loss of 34.51%.

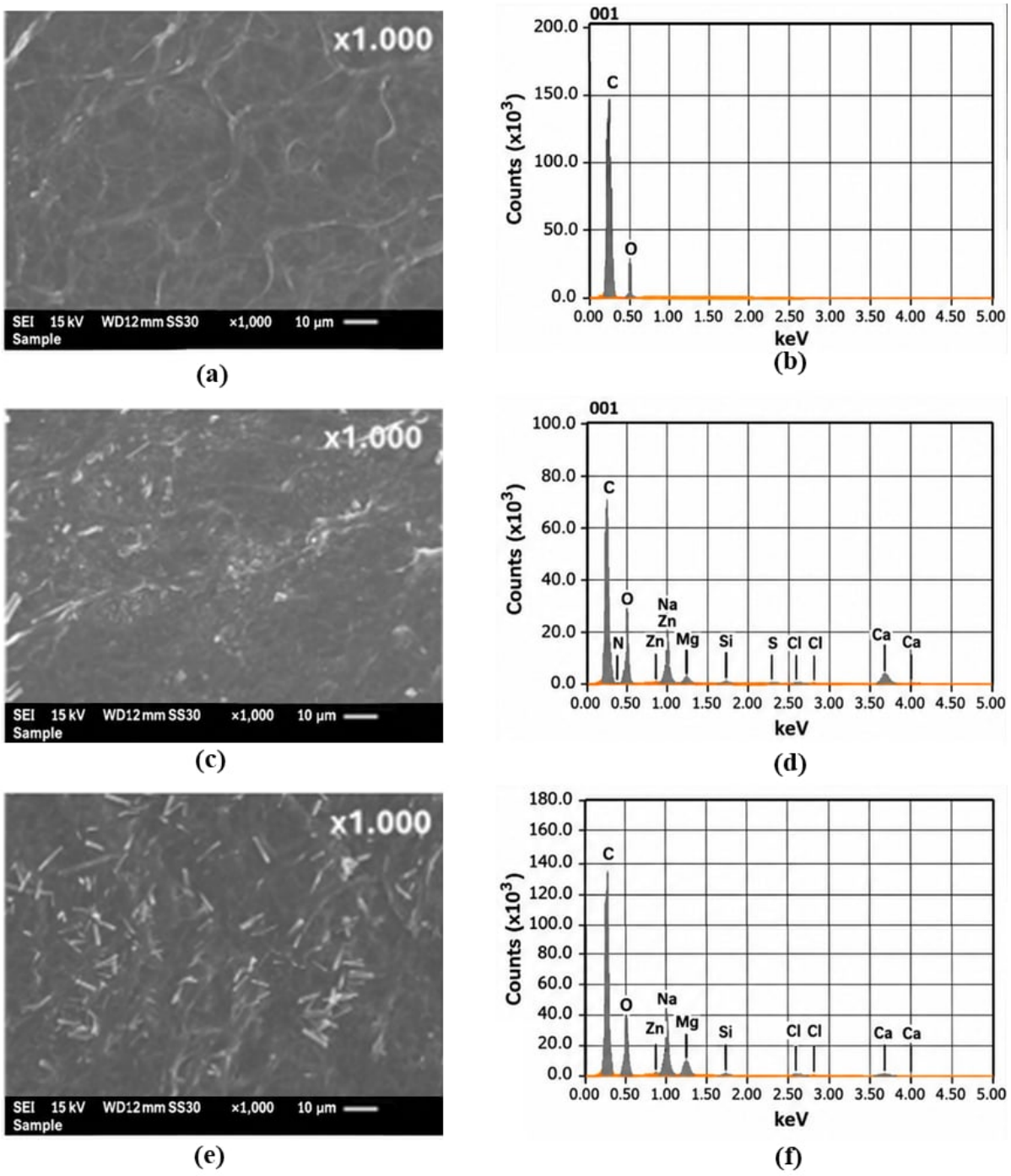

Figure 10. SEM and EDS analyses for MD membranes pristine (**a**,**b**), after use with ROC and cleaning (**c**,**d**), and after use with ROUC and cleaning (**e**,**f**).

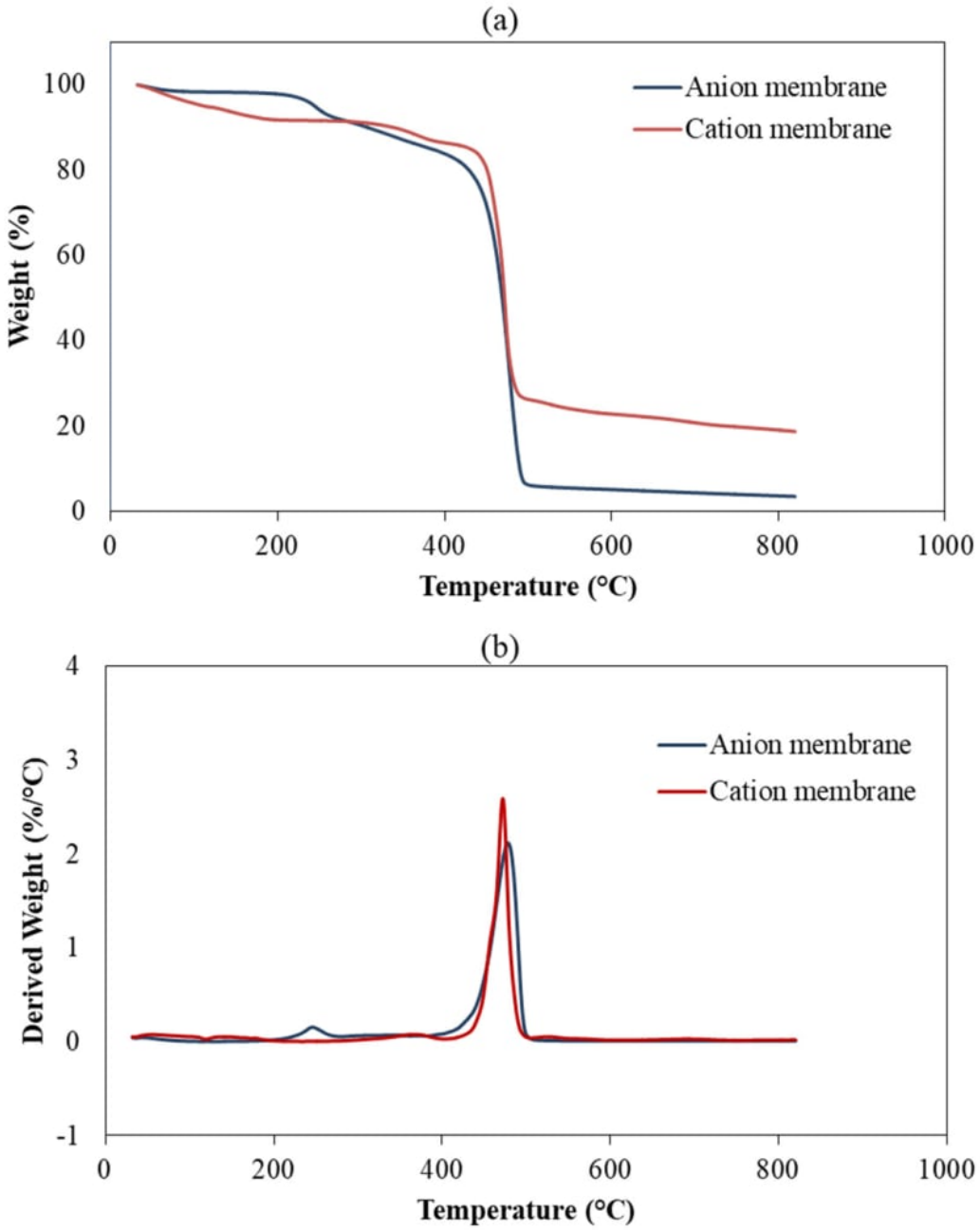

Figure 11. Mass loss (**a**) and derived weight (**b**) for the anion and cation EDI membranes.

Figure 13 presents the mass loss curve (a) and the derived weight (b) for the ROC and ROUC MD membranes. The ROC MD membrane exhibited a total mass loss of 98.2%, corresponding primarily to polymer degradation, with a residual mass of 1.8% attributed to inorganic compounds such as oxides and salts (Figure 13). The ROUC MD membrane showed a 13.2% loss of volatile components, an 83.6% loss associated with the decomposition of organic material, and a 3.2% residual mass, likely resulting from inorganic residues (Figure 13). Polyethylene degradation occurs via random chain scission, thus requiring a higher temperature compared to other polymers [67].

Figure 14 shows the contact angles of the pristine and post-cleaning ROC and ROUC MD membranes. The pristine ROC MD membrane exhibited a contact angle of 118° (Figure 14a), which decreased to 65° after operation and cleaning (Figure 14b), indicating a significant loss of hydrophobicity. Similarly, the pristine ROUC MD membrane showed a contact angle of 60° (Figure 14c), which further decreased to 32° after the experiments

and cleaning (Figure 14d). The reduction in contact angle reflects the persistence of fouling within membrane pores, which is difficult to remove and can cause irreversible wettability [53]. This explains why chemical cleaning was not fully effective in restoring the original hydrophobicity. Membrane fouling is generally unavoidable and remains a major challenge to the large-scale application of MD technology [68]. It typically results from the deposition of inorganic salts such as calcium carbonate ($CaCO_3$), calcium sulfate ($CaSO_4$), and sodium chloride (NaCl), among others [53].

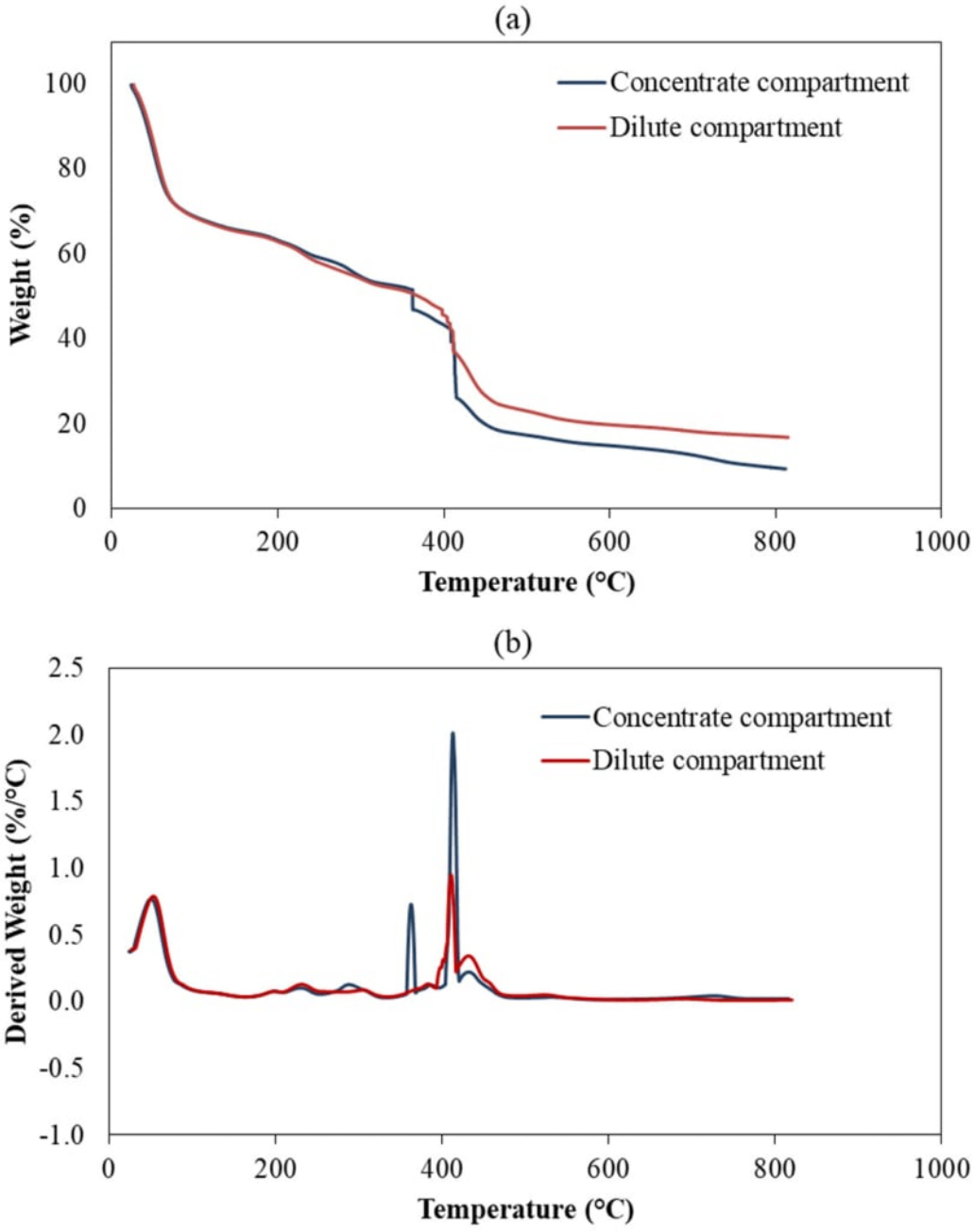

Figure 12. Mass loss (**a**) and derived weight (**b**) for the concentrate and dilute compartments resins.

The surface composition of the anode and cathode after the 5-h EO of MDUC at 50 mA/cm^2, determined by X-ray fluorescence (XRF), is presented in Table 6.

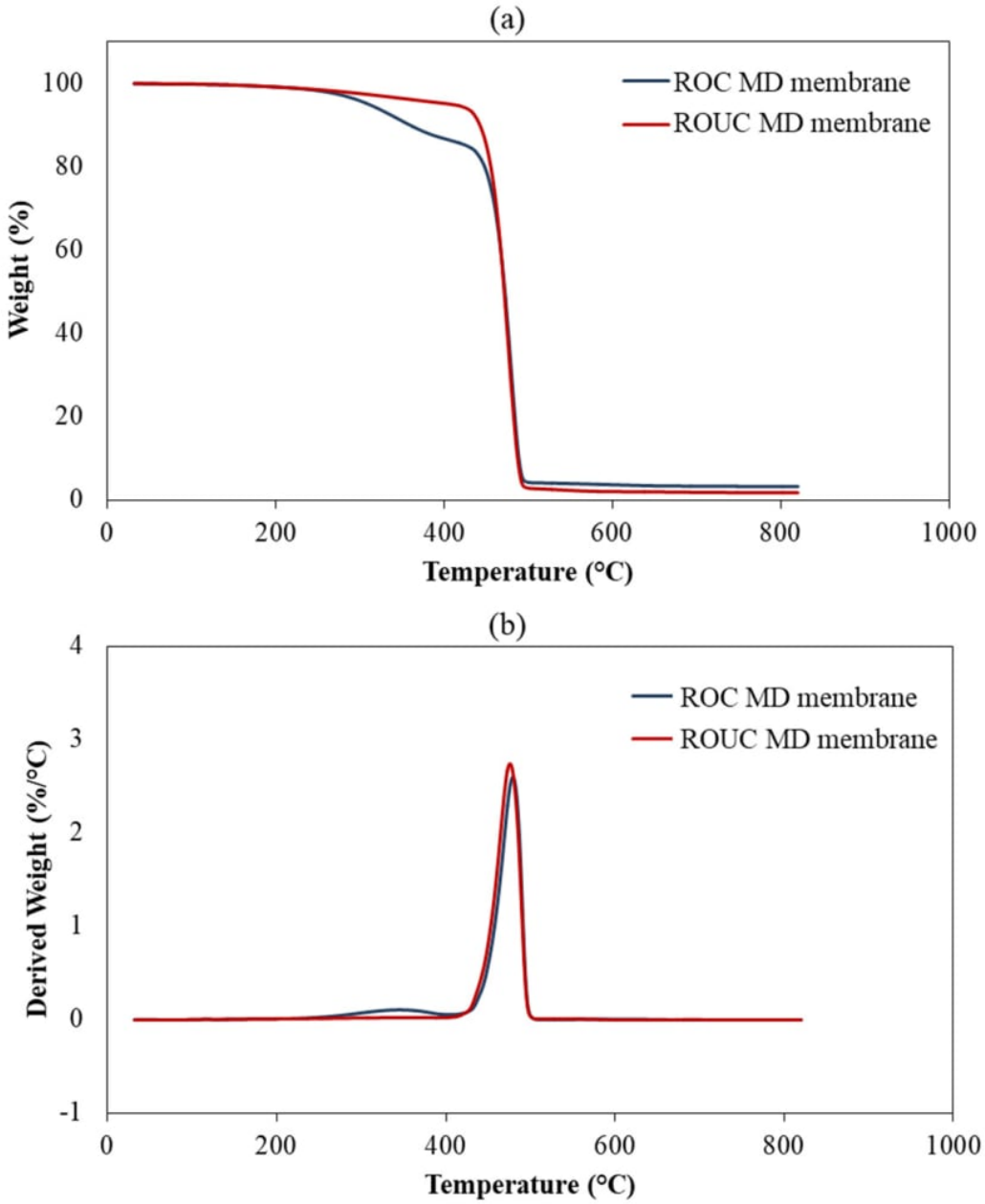

Figure 13. Mass loss (**a**) and derived weight (**b**) for the ROC and ROUC MD membranes.

Several components present in the MDC and MDUC were deposited on the electrode surfaces (Table 6). Titanium was the predominant element, consistent with the electrode material, followed by non-metallic compounds (e.g., sulfates, phosphates) grouped as BAL. Deposits containing magnesium, chlorides, and calcium were also identified. Such precipitation on the electrodes reduces the efficiency of the EO process by physically blocking the active area of the electrode [65]. To mitigate this effect, electrode cleaning can be performed electrochemically (through periodic polarity reversal) or chemically, typically by acid immersion to remove accumulated deposits. In this study, electrochemical cleaning was carried out after 3 h of operation, and visible removal of surface deposits was observed.

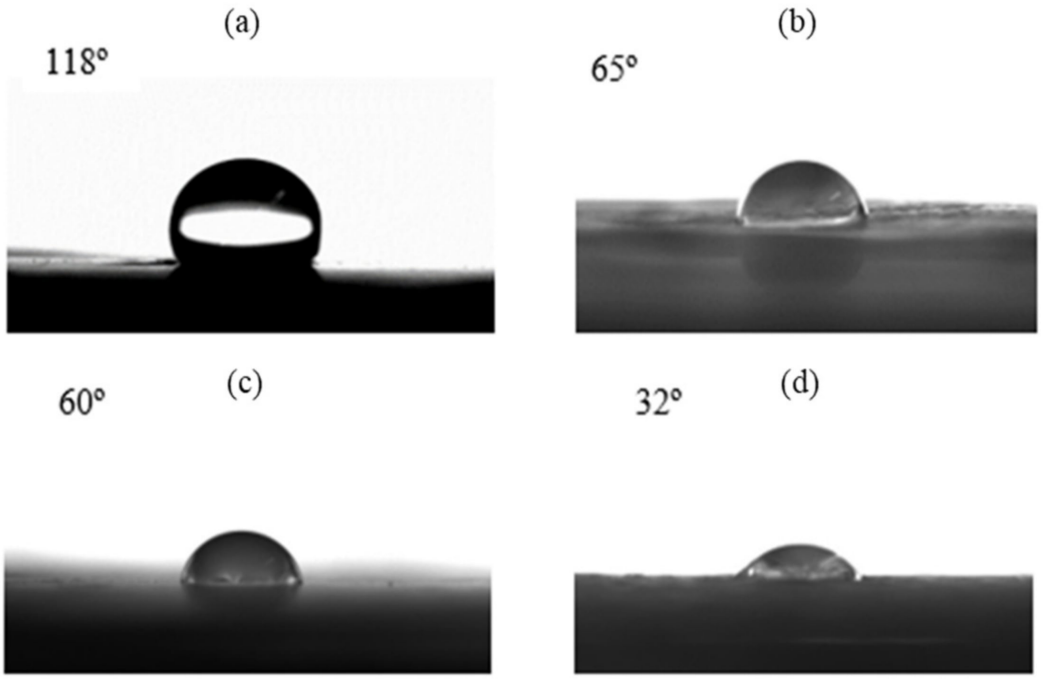

Figure 14. Contact angles of pristine and post-cleaning membranes used in MD experiments with ROC (**a**,**b**) and ROUC (**c**,**d**) feeds.

Table 6. Surface composition of electrodes after 5 h of electro-oxidation (EO) treatment of MDUC at 50 mA/cm^2.

Element	Cathode (ppm)	Anode (ppm)
Titanium	500,417.38	561,455.75
BAL	282,637.09	252,524.58
Magnesium	58,389.36	46,217.29
Phosphorus	50,815.93	48,267.18
Chloride	46,551.89	47,547.14
Calcium	14,259.96	not identified
Aluminum	14,215.85	18,694.45
Sulfur	11,438.99	9471.48
Silicon	5607.96	2808.35
Arsenic	4112.91	3456.55
Tungsten	2739.25	2331.03
Lead	2086.67	1850.41
Copper	1555.94	1353.77
Potassium	812.95	706.81
Selenium	626.49	550.93
Bismuth	413.36	363.32
Silver	386.31	330.95
Barium	318.03	387.93
Palladium	55.06	46.72

3.5. Water Balance of Hybrid Wastewater Treatment Processes

The water balance process for the treatment of ROC is illustrated in Figure 15a, while Figure 15b presents the water balance using ROUC. The analysis begins with the generation of raw wastewater by the petrochemical complex, averaging 706 m^3/h, and follows its progression through conventional treatment and the hybrid system proposed in this study (UF, RO, EDI, MD, and EO).

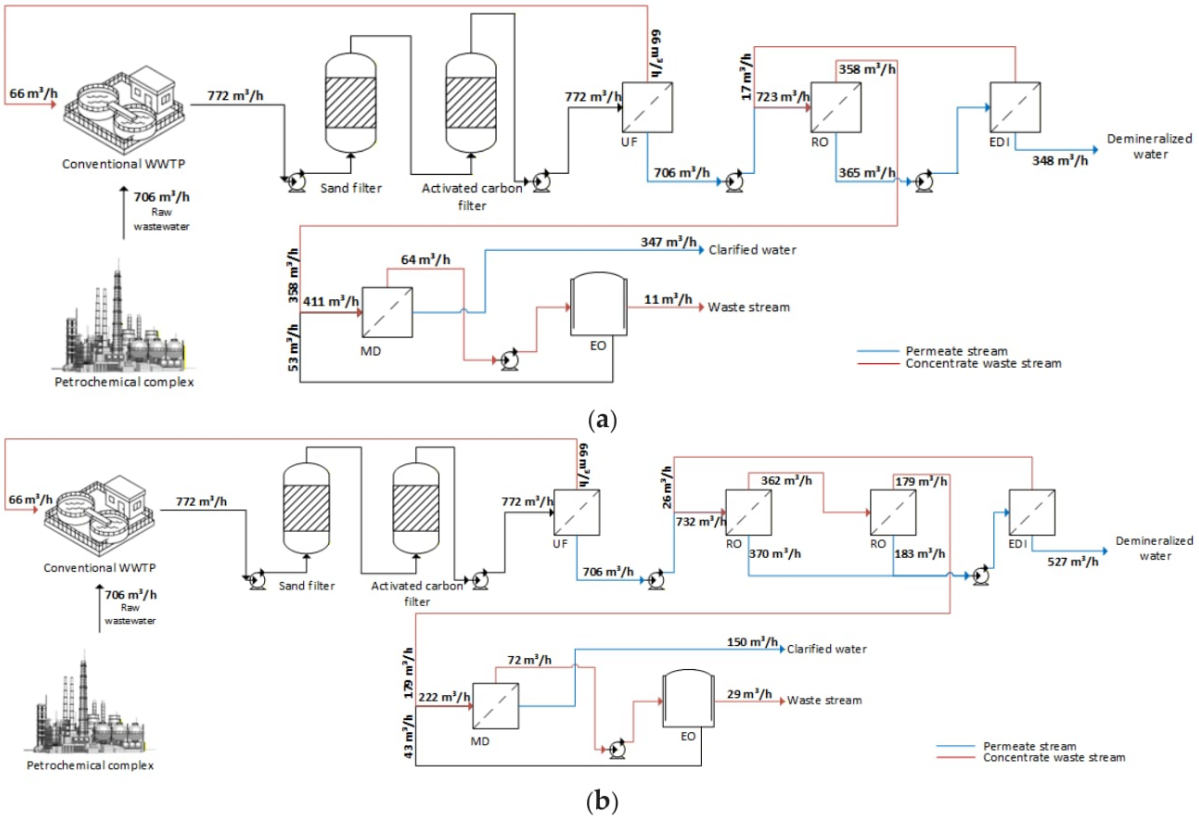

Figure 15. Water balance of the petrochemical wastewater reuse system using ROC (**a**) and ROUC (**b**).

The UF system achieved a recovery rate of 91.5% (Figure 5), producing a 66 m^3/h concentrated stream that was recycled into the activated sludge of the conventional WWTP, and a 706 m^3/h permeate stream. The RO system operated at 50.5% recovery, directing the permeate to the EDI unit and the ROC to the MD unit (Figure 15a). The EDI system achieved 95.3% recovery, generating a 348 m^3/h dilute stream (Figure 15a) that met the quality requirements for reuse as demineralized water, covering approximately 90% of the industries' demineralized water demand. The EDI concentrate was recycled to the RO system.

The ROC was subsequently treated by MD, which achieved 82% recovery (Figure 15a). The MD permeate (347 m^3/h) (Figure 15a) met the criteria for reuse as clarified water and could also be fed to the EDI unit to produce additional demineralized water. Thus, the proposed system using ROC could supply 100% of the petrochemical industry's demineralized water demand, while generating surplus water suitable for use as clarified water. The MD concentrate was treated by EO, and the EO effluent was recycled to the MD unit for another treatment cycle. Overall, the proposed hybrid treatment system using ROC (Figure 15) enables the reuse of approximately 98% of the wastewater generated in the petrochemical complex.

When operating with the ROUC stream (Figure 15b), the EDI system produced 527 m^3/h of demineralized water, exceeding the industry's demand of 389 m^3/h, along with 150 m^3/h of clarified water, achieving an overall wastewater reuse of 96%. The hybrid system using ROC therefore enhances wastewater recovery and optimizes the production of both demineralized and clarified water, compared to ROUC. It can fully meet the industry's demineralized water demand, with 90% supplied by the UF/RO/EDI sequence and the remaining 10% produced from MD permeate via EDI. This integrated treatment approach advances the implementation of a zero-liquid-discharge strategy and supports the transition

from a linear to a circular water management model, reducing both wastewater disposal and freshwater intake by an estimated 6.1 billion liters per year.

The reuse rates achieved with the additional treatment in this study exceed those reported for direct cascade wastewater-reuse systems: Hansen et al. (2018) [69] reported 25.7% wastewater reuse in a Brazilian petrochemical plant; Mohammadnejad et al. (2012) [70] achieved a 26% reduction in freshwater consumption in a refinery in Tehran; Mughees and Al-Ahmad (2015) [71] reported a 38% reduction in water consumption in a gas-processing facility; and Souza et al. (2009) [72] obtained a 17.61% reduction in water consumption in a pulp and paper plant. These results demonstrate that incorporating additional wastewater treatment substantially increases reuse potential.

4. Conclusions

This study demonstrates that integrating UF, RO, EDI, MD, and EO enables highly efficient petrochemical wastewater reuse. The integrated treatment train achieved an overall water recovery of 96 to 98% under the investigated operating conditions, demonstrating substantial potential for wastewater reuse in petrochemical applications. Future studies should focus on economic feasibility, energy consumption, salt accumulation, and concentrate management to assess the long-term sustainability of the proposed system. UF/RO/EDI, already commercially established, reliably produced high-purity demineralized water meeting industrial specifications, while MD and EO effectively valorized RO concentrates, with MD generating clarified water suitable for reuse and EO significantly reducing the organic load and chloride content of MD concentrates. Although the EDI unit achieved high-quality water production during the 24-h test, this operating period was insufficient to assess long-term performance, including potential fouling, resin aging, and operational stability. Therefore, extended testing is recommended to further evaluate the durability and reliability of EDI under continuous operation.

MD performance was limited by membrane wetting and persistent inorganic fouling, and EO showed restricted removal of scale-forming ions, indicating that these steps require further material and process optimization before wide industrial implementation. Advancements such as more robust hydrophobic MD membranes, improved anti-wetting surface designs, and EO configurations with enhanced resistance to scaling could strengthen system stability and reduce lifecycle costs. Overall, the proposed hybrid system offers a viable pathway toward near-zero-liquid-discharge operation, significantly decreasing freshwater demand and waste generation in petrochemical complexes.

Author Contributions: Conceptualization, S.W.d.S., A.V., A.M.B.and M.A.S.R.; Methodology, É.H., M.V.T., A.B.d.S. and M.A.S.R.; Validation, S.W.d.S.; Formal analysis, S.W.d.S., A.V. and A.M.B.; Investigation, É.H., M.V.T. and A.B.d.S.; Resources, S.W.d.S. and M.A.S.R.; Writing—original draft, É.H., M.V.T. and A.B.d.S.; Writing—review & editing, A.V. and A.M.B.; Visualization, P.M.D.A.; Supervision, P.M.D.A., S.W.d.S., A.M.B. and M.A.S.R.; Project administration, P.M.D.A., S.W.d.S. and M.A.S.R.; Funding acquisition, A.M.B. and M.A.S.R. All authors have read and agreed to the published version of the manuscript.

Funding: This research was funded by CNPq (CNPq/BRICS-STI-2-442229/2017-8), RFBR (no. 18-58-80031), CAPES (Finance Code 001), FINEP, FAPERGS, and COFIP.

Data Availability Statement: Data will be made available on request.

Acknowledgments: The funding of CAPES, CNPq, FINEP, FAPERGS, and COFIP is appreciated. Furthermore, the financial support from CNPq (CNPq/BRICS-STI-2-442229/2017-8) and RFBR (no. 18-58-80031) is acknowledged.

Conflicts of Interest: The authors declare no conflicts of interest.

References

1. Zhang, T.; Shen, F.; Peng, X.; Li, Z.; Zhong, W. Carbon-efficient production planning for long-chain integrated refinery-petrochemical processes: A material-energy-carbon optimization perspective. *J. Clean. Prod.* **2023**, *426*, 138916. [CrossRef]
2. Iulianelli, A.; Drioli, E. Membrane engineering: Latest advancements in gas separation and pre-treatment processes, petrochemical industry and refinery, and future perspectives in emerging applications. *Fuel Process. Technol.* **2020**, *206*, 106464. [CrossRef]
3. Han, W.; Gao, Y.; Zhang, G.; Liu, D.; Wu, H.; Fan, L.; Guo, X.; Ji, H.; Zhang, F. Removal of chelated heavy metals from soil washing effluent by a sulfate-reducing bacterium and its re-washing potential. *Environ. Geochem. Health* **2026**, *48*, 271. [CrossRef] [PubMed]
4. Zhao, X.; Zhang, C.; Liu, B.; Zhao, H.; Gao, X.; Wang, Y.; Zhang, Y.; Liu, D.; Wang, C.C. Resource mining from stainless steel pickling wastewater to produce metal-organic frameworks. *Resour. Conserv. Recycl.* **2023**, *188*, 106647. [CrossRef]
5. Nariyoshi, Y.N. Study of fundamentals in membrane distilation crystallization applied for water desalination. *USP* **2016**, *33*, 675–690. [CrossRef]
6. Ronquim, F.M.; Sakamoto, H.M.; Mierzwa, J.C.; Kulay, L.; Seckler, M.M. Eco-efficiency analysis of desalination by precipitation integrated with reverse osmosis for zero liquid discharge in oil refineries. *J. Clean. Prod.* **2020**, *250*, 119547. [CrossRef]
7. Hansen, É.; Rodrigues, M.A.S.; de Aquim, P.M. Characterization of aqueous streams in a petrochemical industry: A study for the reuse of industrial effluents. *J. Water Process Eng.* **2019**, *27*, 99–109. [CrossRef]
8. Merz, N.; Zachariah, M. Understanding droughts under climate change in South America based on severity-duration-frequency curves and drought atlases. *Clim. Change* **2025**, *178*, 163. [CrossRef]
9. Venzke, C.D.; Giacobbo, A.; Ferreira, J.Z.; Bernardes, A.M.; Rodrigues, M.A.S. Increasing water recovery rate of membrane hybrid process on the petrochemical wastewater treatment. *Process Saf. Environ. Prot.* **2018**, *117*, 152–158. [CrossRef]
10. Santos, P.G.; Scherer, C.M.; Fisch, A.G.; Rodrigues, M.A.S. Petrochemical wastewater treatment: Water recovery using membrane distillation. *J. Clean. Prod.* **2020**, *267*, 121985. [CrossRef]
11. Santos, A.B.; Barreto, A.S.; Gonçalves, L.R.; Pires, A.N.; Giacobbo, A.; Rodrigues, M.A.S. Industrial reuse of petrochemical effluents: A case study of ultrafiltration and reverse osmosis. *Cienc. Nat.* **2022**, *44*, e19. [CrossRef]
12. Santos, A.B.; Giacobbo, A.; Rodrigues, M.A.S.; Bernardes, A.M. Integrated membrane process (UF/RO/EDI) for treating a petrochemical wastewater to obtain ultrapure water for industrial reuse. *Process Saf. Environ. Prot.* **2023**, *177*, 223–231. [CrossRef]
13. Gurreri, L.; Tamburini, A.; Cipollina, A.; Micale, G. Electrodialysis applications in wastewater treatment for environmental protection and resources recovery: A systematic review on progress and perspectives. *Membranes* **2020**, *10*, 146. [CrossRef] [PubMed]
14. Wu, Y.; Kang, Y.; Zhang, L.; Qu, D.; Cheng, X.; Feng, L. Performance and fouling mechanism of direct contact membrane distillation (DCMD) treating fermentation wastewater with high organic concentrations. *J. Environ. Sci.* **2018**, *65*, 253–261. [CrossRef]
15. Ali, A.; Quist-Jensen, C.A.; Drioli, E.; Macedonio, F. Evaluation of Integrated Microfiltration and Membrane Distillation/crystallization Processes for Produced Water Treatment. *Desalination* **2018**, *434*, 161–168. [CrossRef]
16. Alessandro, F.; Macedonio, F.; Drioli, E. New Materials and Phenomena in Membrane Distillation. *Chemistry* **2023**, *5*, 65–84. [CrossRef]
17. Venzke, C.D.; Rizzana, D.U.; Giacobbo, A.; Rodrigues, M.A.S.; He, T.; Bernardes, A.M. Membrane distillation treating a real petrochemical reverse osmosis concentrate: Influence of membrane characteristics on the process performance. *J. Water Process Eng.* **2021**, *39*, 101722. [CrossRef]
18. Yin, X.; Li, W.; Zhu, H.; Yu, J.; Wei, K.; Gao, Z.; Zhang, Y.; Chen, H.; Gu, L.; Han, W. Electrochemical treatment of municipal reverse osmosis concentrates by a TiO_2-BNTs/SnO_2-Sb reactive electrochemical membrane. *Sep. Purif. Technol.* **2024**, *331*, 125726. [CrossRef]
19. Fontanova, E.; Grosso, V.; Pantuso, E.; Donato, L.; Profio, G.D. Energy duty in direct contact membrane distillation of hypersaline brines operating at the water-energy nexus. *J. Membr. Sci.* **2023**, *676*, 121585. [CrossRef]
20. Devaisy, S.; Kandasamy, J.; Nguyen, T.V.; Ratnaweera, H.; Vigneswaran, S. Membranes in Water Reclamation: Treatment, Reuse and Concentrate Management. *Membranes* **2023**, *13*, 605. [CrossRef] [PubMed]
21. Xiang, Q.; Nomura, Y.; Fukahori, S.; Mizuno, T.; Tanaka, H.; Fujiwara, T. Innovative Treatment of Organic Contaminants in Reverse Osmosis Concentrate from Water Reuse: A Mini Review. *Curr. Pollut. Rep.* **2019**, *5*, 294–307. [CrossRef]
22. Wang, S.; Qiu, J.; Ren, M.; Cui, Y.; Xie, Y.; Cao, H. Enhanced treatment of reverse osmosis concentrates by ozone micro-nano bubbles coupled with catalytic ceramic membranes. *J. Water Process Eng.* **2024**, *61*, 105213. [CrossRef]
23. Mansour, F.; Alnouri, S.Y.; Al-Hindi, M.; Azizi, F.; Linke, P. Screening and cost assessment strategies for end-of-Pipe Zero Liquid Discharge systems. *J. Clean. Prod.* **2018**, *179*, 460–477. [CrossRef]
24. Venzke, C.D.; Rodrigues, M.A.S.; Giacobbo, A.; Bacher, L.E.; Lemmertz, I.S.; Viegas, C.; Striving, J.; Pozzebon, S. Application of reverse osmosis to petrochemical industry wastewater treatment aimed at water reuse. *Manag. Environ. Qual. Int. J.* **2017**, *28*, 70–77. [CrossRef]

25. Alayande, A.B.; Hong, S. Sulfate radical-based advanced oxidation process for algal toxin mineralization in seawater desalination. *Desalination* **2022**, *539*, 115974. [CrossRef]
26. Ameta, S.C.; Ameta, R. Advanced Oxidation Processes for Waste Water Treatment. In *Emerging Green Chemical Technology*; Academic Press: Cambridge, MA, USA, 2018; pp. i–iii. [CrossRef]
27. Gong, C.; Han, J.; Wu, Y.; He, C.; Zhang, Z.; Hu, Z.; Ren, X. Efficient desalination and synergistic toxic organics removal in RO concentrates with electrochemical advanced oxidation processes. *Desalination* **2024**, *592*, 118205. [CrossRef]
28. Mohammed, S.; Fasnabi, P.A. Removal of dicofol from wastewater using advanced oxidation process. *Procedia Technol.* **2016**, *24*, 645–653. [CrossRef]
29. Richardson, S.D.; Kimura, S.Y. Emerging environmental contaminants: Challenges facing our next generation and potential engineering solutions. *Environ. Technol. Innov.* **2017**, *8*, 40–56. [CrossRef]
30. Albornoz, L.L.; Giacobbo, A.; Guimaraes, R.E.; Da Silva, S.W.; Rodrigues, M.A.S.; Nilson, V.M.; Lazzari, N.H.; Pizzolato, T.M.; Bernandes, A.M. Advanced hybrid systems for wastewater treatment: Integrating nanofiltration and electro-Fenton for pharmaceutical products degradation. *Sep. Purif. Technol.* **2025**, *373*, 133639. [CrossRef]
31. Chen, L.; Li, F.; He, F.; Mao, Y.; Chen, Z.; Wang, Y.; Cai, Z. Membrane distillation combined with electrocoagulation and electrooxidation for the treatment of landfill leachate concentrate. *Sep. Purif. Technol.* **2022**, *291*, 120936. [CrossRef]
32. Illi, J.; Giacobbo, A.; Da Silva, S.W.; Stefens, J.L.; Bernardes, A.M.; Rodrigues, M.A.S. Advanced electrochemical oxidation and membrane distillation for the treatment of landfill leachate concentrated by reverse osmosis. *Sep. Purif. Technol.* **2025**, *370*, 133229. [CrossRef]
33. Li, S.; Zheng, S.; Zheng, X.; Bi, D.; Yang, X.; Luo, X. Optimization of electrolytic system type for industrial reverse osmosis concentrate treatment to achieve effluent quality and energy savings. *Sep. Purif. Technol.* **2022**, *295*, 121343. [CrossRef]
34. ABIQUIM. Yearbook of the Brazilian Chemical Industry. 2025. Available online: https://abiquim.org.br/wp-content/uploads/2026/09/Livreto-Enaiq-2025b.pdf (accessed on 10 October 2026).
35. Kucera, J. Reverse osmosis: Fundamental causes of membrane deposition and approaches to mitigation. In *Water-Formed Deposits Fundamentals and Mitigation Strategies*; Elsevier: Amsterdam, The Netherlands, 2022; pp. 215–237.
36. Urtiaga, A. Electrochemical technologies combined with membrane filtration. *Curr. Opin. Electrochem.* **2021**, *27*, 100691. [CrossRef]
37. *SM 4110 B*; Method 4110 B—Ion Chromatography with Chemical Suppression of Eluent Conductivity. Standard Methods for the Examination of Water and Wasterwater, 23rd ed. American Public Health Association: Washington, DC, USA, 2017.
38. *SM 5220 C*; Method 5220 C—Closed Reflux, Titrimetric Method. Standard Methods for the Examination of Water and Wasterwater, 23rd ed. American Public Health Association: Washington, DC, USA, 2017.
39. *SM 2510*; Method 2510—Conductivity. Standard Methods for the Examination of Water and Wasterwater, 23rd ed. American Public Health Association: Washington, DC, USA, 2017.
40. *SM 3111 B*; Method 3111 B—Direct Air-Acetylene Flame Method. Standard Methods for the Examination of Water and Wasterwater, 23rd ed. American Public Health Association: Washington, DC, USA, 2017.
41. *SM 4500 H+*; Method 4500 H+—pH Value. Standard Methods for the Examination of Water and Wasterwater, 23rd ed. American Public Health Association: Washington, DC, USA, 2017.
42. *SM 3500 KB*; Method 3500 KB—Flame Photometric Method. Standard Methods for the Examination of Water and Wasterwater, 23rd ed. American Public Health Association: Washington, DC, USA, 2017.
43. *SM 3500 NaB*; Method 3500 NaB—Flame Emission Photometric Method. Standard Methods for the Examination of Water and Wasterwater, 23rd ed. American Public Health Association: Washington, DC, USA, 2017.
44. *SM 2540 B*; Method 2540 D—Total Solids Dried at 103–105 °C. Standard Methods for the Examination of Water and Wasterwater, 23rd ed. American Public Health Association: Washington, DC, USA, 2017.
45. *SM 2130 B*; Method 2130 B—Nephelometric Method. Standard Methods for the Examination of Water and Wasterwater, 23rd ed. American Public Health Association: Washington, DC, USA, 2017.
46. *SM 2540 D*; Method 2540 D—Total Suspended Solids Dried at 103–105 °C. Standard Methods for the Examination of Water and Wasterwater, 23rd ed. American Public Health Association: Washington, DC, USA, 2017.
47. *ASTM E1131-20*; Standard Test Method for Compositional Analysis by Thermogravimetry. ASTM International: West Conshohocken, PA, USA, 2020.
48. Widiasa, I.N.; Susanto, A.A.; Susanto, H. Performance of an integrated membrane pilot plant for wastewater reuse: Case study of oil refinery plant in Indonesia. *Desalin. Water Treat.* **2014**, *52*, 7443–7449. [CrossRef]
49. Jafarinejad, S. A comprehensive study on the application of reverse osmosis (RO) technology for the petroleum industry wastewater treatment. *J. Water Environ. Nanotechnol.* **2017**, *2*, 243–264. [CrossRef]
50. Wood, J.; Gifford, J.; Arba, J.; Shaw, M. Production of ultrapure water by continuous electrodeionization. *Desalination* **2010**, *250*, 973–976. [CrossRef]
51. Qasim, M.; Badrelzaman, M.; Darwish, N.N.; Darwish, N.A.; Hilal, N. Reverse osmosis desalination: A state-of-the-art review. *Desalination* **2019**, *459*, 59–104. [CrossRef]

52. Jiang, B.; Zhang, X.; Zhao, X.; Li, F. Removal of high level boron in aqueous solutions using continuous electrodeionization (CEDI). *Sep. Purif. Technol.* **2018**, *192*, 297–301. [CrossRef]
53. Wang, S.; You, Y.; Wang, X.; Huang, W.; Zheng, L.; Li, F. Fouling mechanism and effective cleaning strategies for vacuum membrane distillation in brackish water treatment. *Desalination* **2023**, *565*, 116884. [CrossRef]
54. Chen, L.; Xu, P.; Wang, H. Interplay of the Factors Affecting Water Flux and Salt Rejection in Membrane Distillation: A State-of-the-Art Critical Review. *Water* **2020**, *12*, 2841. [CrossRef]
55. Hernon, B.P.; Zanapalidou, R.H.; Zhang, L.; Sims, K.J.; Siwak, L.R. *Electrodeionization in Power Plant Applications*; GE Technical Paper; GE Research: Niskayuna, NY, USA, 2010.
56. Nadjafi, M.; Reyhani, A.; Al Arni, S. Feasibility of treatment of refinery wastewater by a pilot scale MF/UF and UF/RO system for reuse at boilers and cooling towers. *J. Water Chem. Technol.* **2018**, *40*, 167–176. [CrossRef]
57. Wood, J.; Gifford, J. *Continuous Electrodeionization*; John Wiley & Sons, Inc.: Hoboken, NJ, USA, 2019; pp. 287–328. [CrossRef]
58. Chaturvedi, S.; Dave, P.N. Removal of iron for safe drinking water. *Desalination* **2012**, *303*, 1–11. [CrossRef]
59. Katsoyiannis, I.A.; Gkotsis, P.; Castellana, M.; Cartechini, F.; Zouboulis, A.I. Production of demineralized water for use in thermal power stations by advanced treatment of secondary wastewater effluent. *J. Environ. Manag.* **2017**, *190*, 132–139. [CrossRef] [PubMed]
60. Silva, S.W.; Venzke, C.D.; Welter, J.B.; Schneider, D.E.; Ferreira, J.Z.; Rodrigues, M.A.S.; Bernardes, A.M. Electrooxidation Using Nb/BDD as Post-Treatment of a Reverse Osmosis Concentrate in the Petrochemical Industry. *Int. J. Environ. Res. Public Health* **2019**, *16*, 816. [CrossRef] [PubMed]
61. Martínez-Huitle, C.A.; Rodrigo, M.A.; Sirés, I.; Scialdone, O. Single and Coupled Electrochemical Processes and Reactors for the Abatement of Organic Water Pollutants: A Critical Review. *Chem. Rev.* **2015**, *115*, 13362–13407. [CrossRef] [PubMed]
62. Zhao, C.; Wu, Z.; Lai, J.; Liu, L.; Li, H.; Wang, H. Efficient electrochemical oxidation of refractory organics in actual petrochemical reverse osmosis concentrates by Ti/SnO2-Sb mesh anode. *Process Saf. Environ. Prot.* **2024**, *182*, 1060–1071. [CrossRef]
63. Bard, A.J.; Faulkner, L.R.; White, H.S. *Electrochemical Methods: Fundamentals and Applications*, 3rd ed.; Wiley: Hoboken, NJ, USA, 2022; p. 1104.
64. Silva, S.W.; Klauck, C.R.; Rodrigues, M.A.S.; Bernardes, A.M. Degradation of the commercial surfactant nonylphenol ethoxylate by advanced oxidation processes. *J. Hazard. Mater.* **2015**, *282*, 241–248. [CrossRef] [PubMed]
65. Moreira, F.V.; Boaventura, R.A.R.; Brillas, E.; Vilar, V.J.P. Electrochemical advanced oxidation processes: A review on their application to synthetic and real wastewaters. *Appl. Catal. B Environ.* **2017**, *202*, 217–261. [CrossRef]
66. Zhang, Z.; Du, X.; Carlson, K.H.; Robbins, C.A.; Tong, T. Effective Treatment of Shale Oil and Gas Produced Water by Membrane Distillation Coupled with Precipitative Softening and Walnut Shell Filtration. *Desalination* **2019**, *454*, 82–90. [CrossRef]
67. Miandad, R.; Rehan, M.; Barakat, M.A.; Aburiazaiza, A.S.; Khan, H.; Ismail, I.M.I.; Dhavamani, J.; Gardy, J.; Hassanpour, A.; Nizami, A.S.N. Catalytic Pyrolysis of Plastic Waste: Moving Toward Pyrolysis Based Biorefineries. *Front. Energy Res.* **2019**, *7*, 27. [CrossRef]
68. Zhang, Y.; Guo, F. Mitigating near-surface polarizations in membrane distillation via membrane surface decoration. *Desalination* **2024**, *579*, 117507. [CrossRef]
69. Hansen, E.; Rodrigues, M.A.S.; Aragão, M.E.; Aquim, P.M. Water and wastewater minimization in a petrochemical industry through mathematical programming. *J. Clean. Prod.* **2018**, *172*, 1814–1822. [CrossRef]
70. Mohammadnejad, S.; Ataei, A.; Bidhendi, G.R.N.; Mehrdadi, N.; Ebadati, F.; Lotfi, F. Water pinch analysis for water and wastewater minimization in Tehran oil refinery considering three contaminants. *Environ. Monit. Assess.* **2012**, *184*, 2709–2728. [CrossRef] [PubMed]
71. Mughees, W.; Al-Ahmad, M. Application of water pinch technology in minimization of water consumption at a refinery. *Comput. Chem. Eng.* **2015**, *73*, 34–42. [CrossRef]
72. Souza, A.A.; Forgiarini, E.; Brandão, H.L.; Xavier, M.F.; Pessoa, F.L.P.; Souza, S.G.U. Application of Water Source Diagram (WSD) method for the reduction of water consumption in petroleum refineries. *Resour. Conserv. Recycl.* **2009**, *53*, 149–154. [CrossRef]

Disclaimer/Publisher's Note: The statements, opinions and data contained in all publications are solely those of the individual author(s) and contributor(s) and not of MDPI and/or the editor(s). MDPI and/or the editor(s) disclaim responsibility for any injury to people or property resulting from any ideas, methods, instructions or products referred to in the content.